ANALYSIS OF CYCLONE SEPARATOR USING CFD METHODOLOGY

A DISSERTATION

SUBMITTED IN PARTIAL FULFILMENT OF THE REQUIREMENTS FOR THE AWARD OF THE DEGREE OF

MASTER OF TECHNOLOGY

IN

ENVIRONMENTAL ENGINEERING

Submitted By

Mayank Chetiwal

ROLL NO. 2K16/ENE/12

Under The Supervision Of

DR BHARAT JHAMNANI

(Assistant Professor)

DEPARTMENT OF ENVIRONMENTAL ENGINEERING

DELHI TECHNOLOGICAL UNIVERSITY

(Formerly Delhi College of Engineering)

Bawana Road, Delhi-110042

JULY, 2018

DELHI TECHNOLOGICAL UNIVERSITY

(Formerly Delhi College of Engineering)

Bawana Road, Delhi-110042

CANDIDATE'S DECLARATION

I Mayank Chetiwal, 2K16/ENE/12 student of M. Tech, Environmental Engineering, hereby declare that the project Dissertation title "Analysis of Cyclone Separator using CFD methodology" which is submitted by me to the Department of Environmental Engineering, Delhi Technological University, Delhi in partial fulfilment of the requirement for the award of the degree of Master of Technology, is original and not copied from any source without proper citation. This work has not previously formed the basis for the award of any Degree, Diploma associateship, Fellowship or other similar title or recognition.

Place: Delhi (MAYANK CHETIWAL)

Date: 20 July 2018

ENVIRONMENTAL ENGINEERING DEPARTMENT

DELHI TECHNOLOGICAL UNIVERSITY

(Formerly Delhi College of Engineering)

Bawana Road, Delhi-110042

CERTIFICATE

I hereby certify that the Project Dissertation titled "Analysis of Cyclone Separator using CFD methodology" which is submitted by Mayank Chetiwal, Roll No. 2K16/ENE/12, Department of Environmental Engineering, Delhi Technological University, Delhi in partial fulfillment of the requirement for the award of the degree of Master of Technology, is a record of the project work carried out by the students under my supervision. To the best of my knowledge this work has not been submitted in part or full for any Degree or Diploma to this University or elsewhere.

Place: Delhi (DR. BHARAT JHAMNANI)

Date: SUPERVISOR

ACKNOWLEDGEMENT

It is a great pleasure to have the opportunity to extend my heartiest gratitude to everybody who helped me throughout this thesis. It is distinct pleasure to express my deep sense of gratitude and indebtedness to my learned supervisors **Dr. Bharat Jhamnani** in the Department of Environmental Engineering, Delhi Technological University for their invaluable guidance, encouragement, and patient review. His continuous inspiration has enabled me to complete this major project.

I would also like to take this opportunity to present our sincere regards to my Head of the Department **Prof. S. K. Singh** for his kind support and encouragement. I am thankful to my family members, friends and classmates for their unconditional support and motivation.

MAYANK CHETIWAL

ROLL NO. 2K16/ENE/12

ABSTRACT

The Particulate Matter is the most crucial parameter which decides the pollution level in air. The negative impact of particulate matter is solely because of its submicron size which causes bad effects on human. There are many air quality control devices available which separates out the particulate matter using different sets of principles. Cyclone Separator is a type of air quality control device which uses physical phenomenon of centrifugal acceleration. The efficiency of cyclone separator to eliminate particulate matter is average as compared to other devices and techniques but its cost efficiency is quite high due to its basic working principle and no moving parts. The polluted air enters tangentially from the inlet and descends in swirling pattern in the hollow cylinder and cone parts of the cyclone body. This spiral motion of particle laden air produces a centrifugal force on the particles and pushes them towards wall of the cyclone. Therefore, the designing and analysis of cyclone separator is difficult due to complex flow pattern.

Pressure drop and different velocities generated through cyclone body is the most important parameter to predict its performance. Many studies and research work have been done in the field of cyclone separator but there are no specific techniques and empirical formulas to analyse the flow pattern and pressure drop. Solving the flow and particle transport equations using CFD (Computational Fluid Dynamics) approach is one of the method that can be followed with specific sets of equations and model.

The present study is carried out to analyse the performance of three models of cyclone separator with different vortex finder diameter using RSM (Reynolds stress model) methodology to predict turbulent flow behaviour and DPM (Discrete phase model) to trace the particles trajectories through each cyclone model. The equations are solved computationally using the CFD based software FLUENT (v18.2). The case in the study is computed using an assumption of one-way coupling in the cyclone separator. The graphs and contours of velocities and pressure drop are analysed and compared to study the effect of varying diameter of vortex finder. Collection efficiency is determined by injecting a fixed number of particles from inlet and counting the trapped particles.

Table of Contents

Contents

List of figures

List of Tables

LIST OF SYMBOLS, ABBREVIATIONS AND NOMENCLATURE

a	cyclone inlet height, [m]
b	cyclone inlet width, [m]
C_D	drag coefficient, [–]
C_{pt}	total pressure loss coefficient
C_μ	constant, [–]
d_p	particle diameter, [m]
D	cyclone diameter, [m]
D_c	cone-tip diameter, [m]
D_x	exit pipe diameter, [m]
E	empirical constants, [–]
g	gravity acceleration vector, [m/s^2]
h	height of cyclone cylinder part, [m]
h_c	height of cyclone conical part, [m]
L_h	height of cyclone hopper, [m]
L_e	length of cylindrical barrel top, [m]
K	turbulent kinetic energy, [m^2/s^2]
P	mean pressure, [Pa]
P_t	local total pressure, [Pa]
R	cyclone radius, [m]
P_{t1}	inlet total pressure, [Pa]
Re	cyclone Reynolds number, [–]
Re_p	particle relative Reynolds number, [–]
S	exit pipe length in the interior of the cyclone,[m]
u_i	mean velocity in i-direction, [m/s]
u_j	mean velocity in j-direction, [m/s]
u_x u_y u_z	fluctuating velocities, [m/s]
U	fluid velocity, [m/s]
U_o	inlet velocity, [m/s]
x	distance along cyclone radius, [m]
y	normal distance to the wall, [m]
κ	Von Karman constant, [-]
τ_w	viscosity of the gas, [Pa]

CHAPTER 1

INTRODUCTION

Air is one of the four classical elements namely *air, water, fire and earth* which are most vital for survival of any living beings. Nature gifted us an extremely precise mixture of gases in certain proportion which makes the life possible here on earth. Air also consists of several tiny dust particles which always remain in continuous suspension within air. However, the air we breathe is getting polluted due to irresponsible and self-centred behaviour of men. Air pollution is a collective term given to the diffusion of toxic and unwanted substance in fresh air which causes serious health threats to the health of living organisms including plants, animals and human beings. This chapter is to throw a bright light on air pollution and its constituents.

1.1 AIR POLLUTION AT GLANCE

Air pollution is one of the major environmental problem which the world is facing nowadays. There are mainly human activities and self-centredness behind this rapidly increasing of air pollution rate. Air pollution is mainly contributed by automobiles, transportation activities industrialization and construction activities. The emission of several toxic gases or hazardous elements from the sources is causing the whole atmospheric and climatic dis-alignment. Ozone hole is one of an example of growing air pollution which causes alarming instabilities in the environment. High demand of resource and natural assets consumption by rapidly growing human population is the chief cause of this kind of pollution. These uncontrolled human activities causing hazardous substances to mix with the clean air and making our atmosphere polluted than ever. Also, it's forcing the climate change in a negative way and causing huge impacts such as global warming. Industrial processes release many detrimental elements like toxic gasses, contaminant such as lead and cadmium, carbon monoxide, carbon dioxide and other substances to the atmosphere. According to World Health Organization report in 2014, air pollution in 2012 caused the deaths of as many as 7 million people globally. It is an estimate roughly resonated by the International Energy Agency.

A pollutant can be of naturally originated or man-made. Pollutants are classified as primary and secondary. Primary pollutants are mainly originated from a single process or source. On the other hand, secondary pollutants are not released directly from a single point source but they form in the air when primary pollutants interact with atmospheric agencies. Formation of **Ground level ozone** is a prominent example of a secondary pollutant. However, some pollutant can have both the characteristics of primary and secondary pollutants as they can be emitted directly and forms from other primary pollutants also.

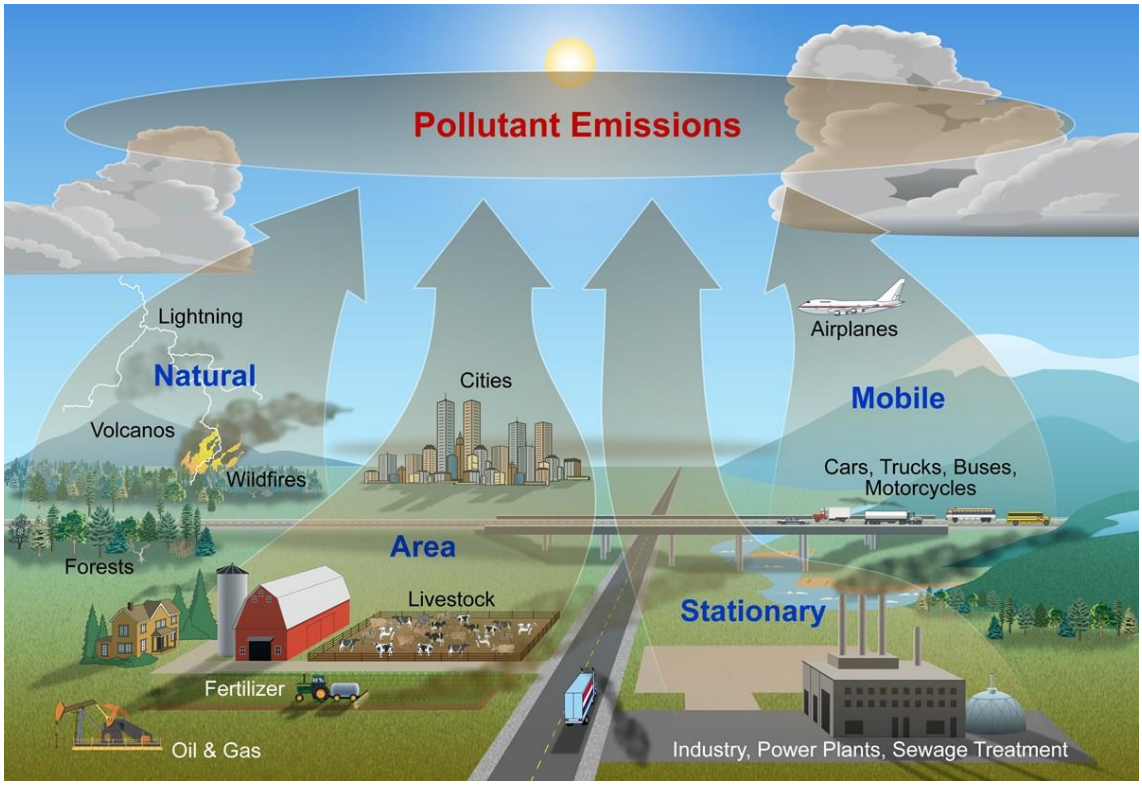

Figure 1.1: A picture showing various sources of air pollution

1.2 PARTICULATE MATTER AND AEROSOLS

Particulate matter is a collective term given to several tiny particles. It is basically a mixture of solid and liquid particles suspended in air. A wide portion of Particulate Matter is hazardous to humans and animals. This unpredictable blend incorporates both natural and inorganic particles. A few cases of particulate matter is dust, ash, smoke, and liquid drops. These particles vacillate enormously in size and composition. Also

aerosol is a term given to the suspension of fine particles of solid or fluid, especially in air or another gas. It can be of natural or anthropogenic inception. Steam, haze, timberland exudates and dust are few of the cases of aerosol has natural origin and whereas fog, particulate matter, smoke and smog are some cases of anthropogenic aerosol.

1.2.1 Size Distribution of Atmospheric Diffused Particles

Size of diffused particles in atmosphere has a wide range and it is measured on the basics of their aerodynamic diameter. Its measurement unit is in microns or micrometre (10^{-6} meter). They are further divided into two categories stated as **inhalable** and **non-inhalable.** Non-inhalable matter is the one which has size range greater than 10 microns. Whereas, the inhalable particles have size range less than 10 microns aka *Particulate Matter*.

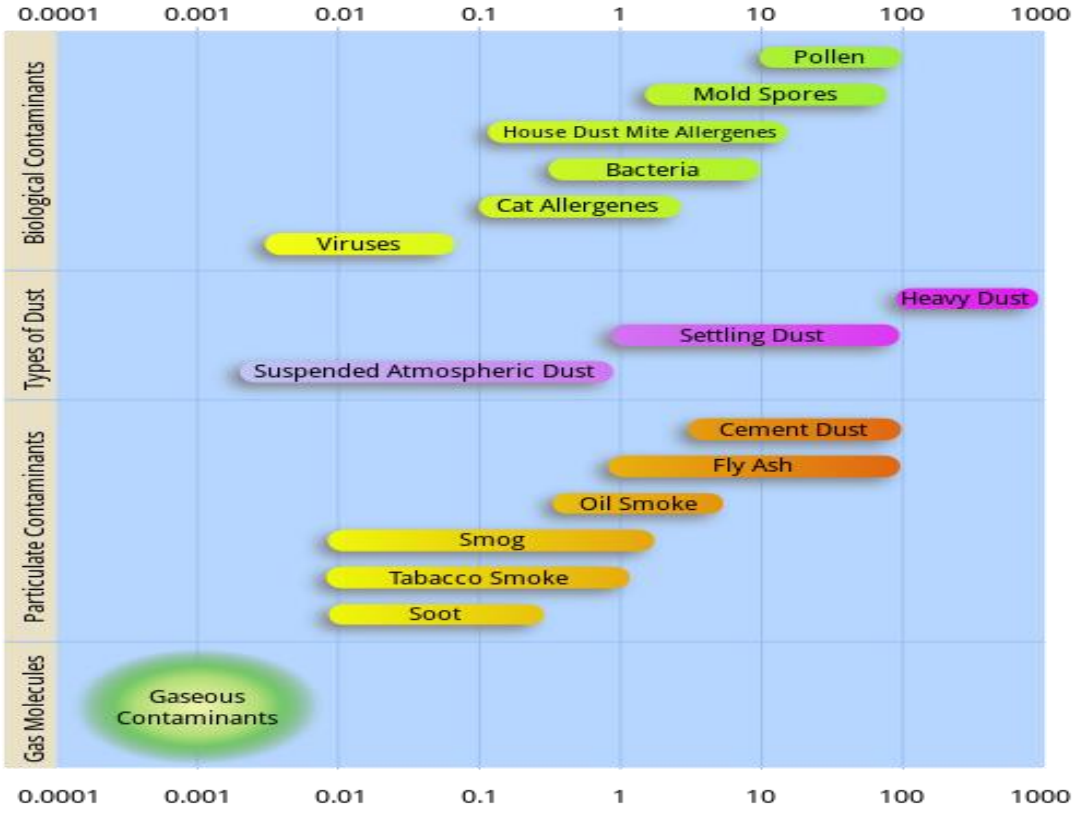

Figure 1.2: a picture showing different size ranges of particulate matter

To have a clear picture of the size distribution, one can consider an example of human hair. The thickness of human hair has size ranges between 50-70 microns which is 30 to 40 times larger than the biggest size of inhalable particulate matter.

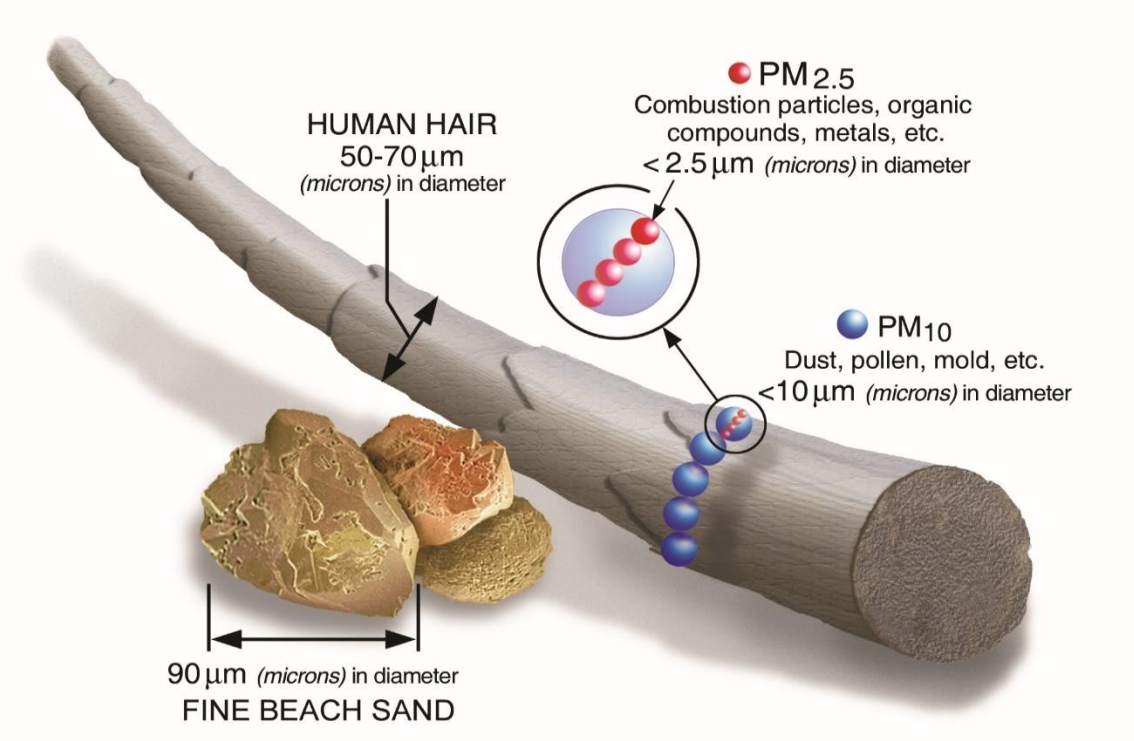

Figure 1.3: Comparison of human hair and inhalable particulate matter (source: USEPA official website)

1.2.2 EFFECTS OF PARTICULATE MATTER

a) Health Effects

The size of particles is specifically responsible for the potential medical issues. Particles under the size range of 10 microns in diameter has an extraordinary potential to cause fatal respiratory issues since they can enter into individual's lungs through air, and even get into his/her circulation system.

Contact with such small particles can affect both lungs and heart in a many ways. Abundance of scientific studies has shown the links of particulate matter pollution exposure to a variety of health problems, such as:

- Small and non-fatal heart attacks
- Uneven heartbeat
- Aggressive or severe asthma

- Lessened lung functioning
- Growth in respiratory symptoms, such as irritation in the windpipe, coughing or difficulty in breathing.

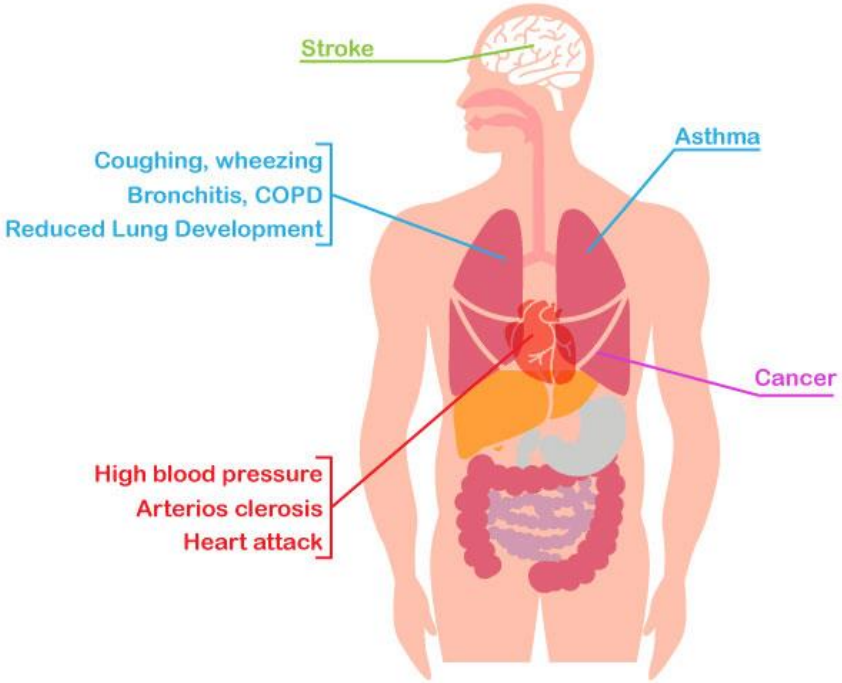

Figure 1.4: Figure explaining various effects of Particulate Matter on Human body

The group of $PM_{2.5}$, have smaller diameters but greater surface areas and therefore can carry various toxic elements along with them. They pass through the filtration from nose hair more easily as compared to PM_{10}. They can reach at the end of the respiratory system with the breathing air and get accumulated there by time passes. It can damage the other parts of the body also by the air exchange from the lungs. Adults exposed to high levels of ambient air pollution, for example PM_{10} and coarse particulate matter, have shown a peak increase in prevalence of respiratory disease.

b) Environmental Effects

Wind carries the particulate matter to far distances and it get deposited on the ground. Depending on the chemical and physical composition, following effects can prevail:

- Decreasing the pH levels of lakes and streams
- Altering the nutrient balance in coastal water-bodies and river basins
- Depleting the nutrients from soil
- Damaging delicate forests and crops
- Affecting the diversity and ecological balance of ecosystems
- Contributing to acidic rain

1.3 SOURCES OF PARTICULATE MATTER

The main sources of primary PM are consequent from both human and natural activities but the substantial portion of PM sources is generated via human (anthropogenic) sources. These activities incorporate farming work, industrial work, burning of wood and other petroleum derivatives, development and devastation exercises, entrainment of street dust into the air and many more.. Natural (non-anthropogenic) sources and phenomenon also contribute to this overall PM problem such as dust storm, windblown and wildfires.

Secondary air pollutant sources emit air contaminants into the atmosphere which forms or help in forming the PM. In this context, these pollutants are considered as predecessors to PM formation. These secondary pollutants mainly are SO_x , NO_x, VOCs, and ammonia. Controlling and eliminating measures that reduce PM forerunners emission tend to have a positive impact on ambient PM levels.

"My concentration in this study will be on the anthropogenic sources. I will analyse mainly the industrial processes in which high concentration of PM is generated".

1.4 CONTROLLING TECHNOLOGIES

Particulate Matter emissions are highly taken care in most of the industrialized countries as the high production rate. Due to various environmental apprehensions, most of the industries are required to operate some short of dust and gas collection arrangement to control particulate and other toxic gas emissions. This system includes:

- Inertial collectors aka cyclonic separators
- Fabric filter collectors or bag-houses
- Wet scrubbers
- Electrostatic precipitators

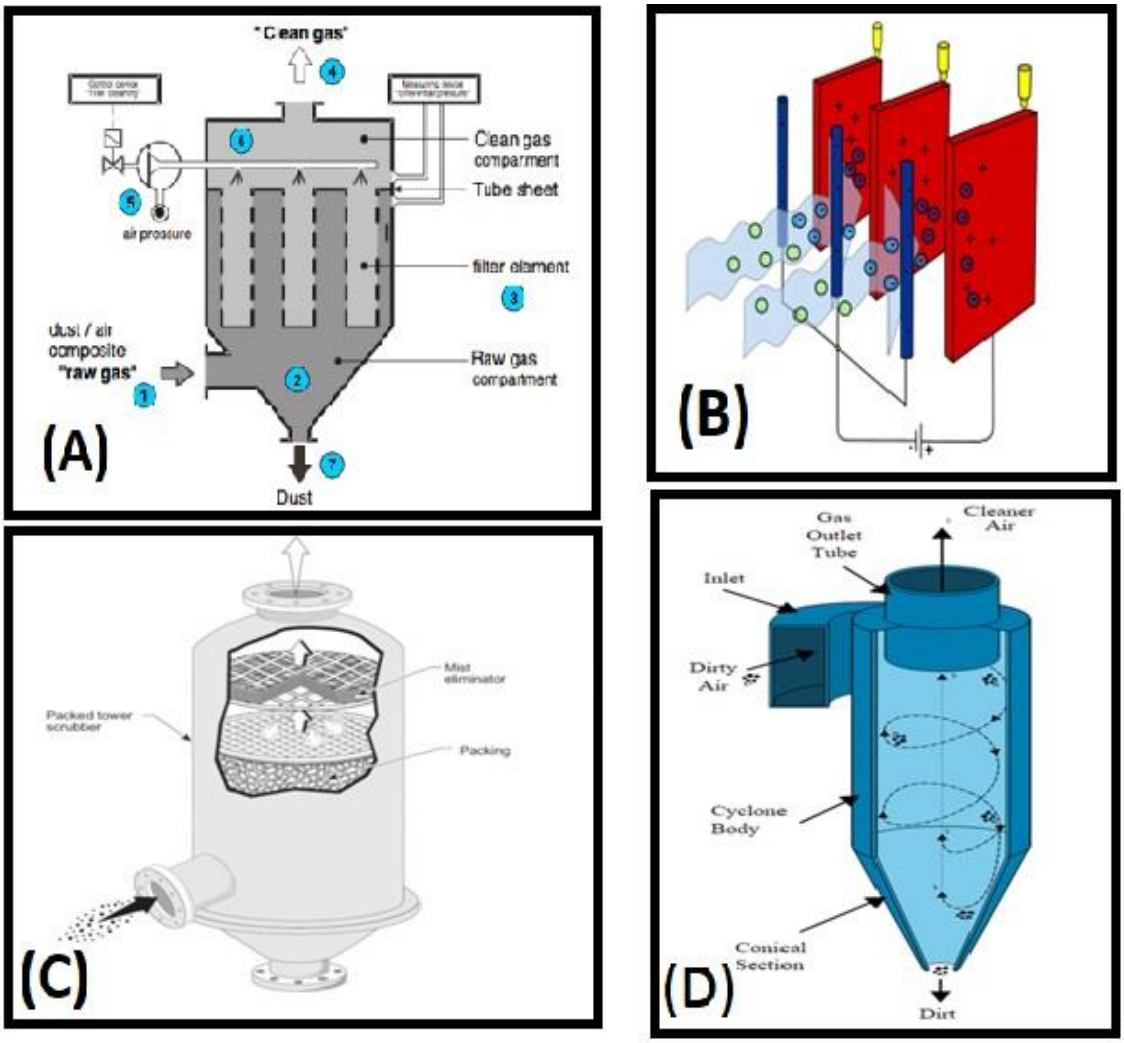

Figure 1.5: showing a variety of dust separators namely (A) Baghouse or fabric fillers (B) Electrostatic Precipitator (C) Wet Scrubbers and (D) Cyclonic Separator

1.5 CYCLONE SEPARATOR

Cyclone separator is one of the most widely used air pollution control devices and also known as pre-cleaners. They commonly remove large size-range of particulate matter. Cyclone Separator is a suspended matter removal device with no moving parts and works on the principle of centrifugal separation of dust particles from the polluted gaseous stream or liquid stream. It portrays the motion of cyclone as it name suggests, to exclude out the dust particles from the gaseous stream. They are usually designed for PM range above 10 micron as it prevents finer filtration techniques to deal with the larger and rough particles later in the cleaning process. It is quite efficiently provides a better method of removing particulate matter from the particle laden stream at low cost and maintenance. Cyclones are fairly more muddled and complex in design than simple gravity settling chambers however their expulsion proficiency is obviously better than

Figure1.6: Picture of Industrial cyclonic separator

that of settling chamber. But they are not always designed as a pre-treatment device. Many modifications and designing techniques can be used to optimize a Cyclone Separator with high efficiency in removing PM_{10} and smaller at low cost. This type of cyclone is called **Super Cyclone** because of its high separation efficiency and more removal of finer particles.

Figure 1.7: A Cyclone Separator installed in a factory (source: Google)

1.5.1 Basic Geometry and Working Principle

The cyclone separators work on a simple principle of centrifugal-separation. It comprises of an upper cylindrical and hollow part known as barrel and a lower conical part signified to as cone which helps in the formation of vortex in the cyclone. They basically change the inertial force of gas particle to a centrifugal force by means of a vortex formation in the cyclone body. The contaminated gas stream with particles enters extraneously from inlet which is situated at the highest point of the cylindrical barrel. In the wake of entering, it descends into the conical area in spiral pattern forming an outer vortex. As the air velocity increases in the outer vortex due to geometry transition, a centrifugal force on the particles which separates them from the air stream starts acting on them. When the air finally reaches at the bottom of the conical part, it begins to flow radially inwards and out the top as clean air. The pollutants fall into the **dust collector** chamber attached to the bottom of the cyclone. Cyclone Separator is a conventional tool

and being used for many decades. It's quite popular device for separating particles because of its simple working and efficient collection rate. Cyclone Separator can be considered as a special type of settling chamber for discrete particles with strong centrifugal force acting on them instead of gravitational force. They can be classified in terms of physical state of two phases. These phases can be **gas-solid, gas-liquid, liquid-solid and liquid-liquid** (Svarovski, 1984).The one with the liquid phase included are also known as **Hydro-cyclone**. This thesis will be limited to the **gas-solid** phase.

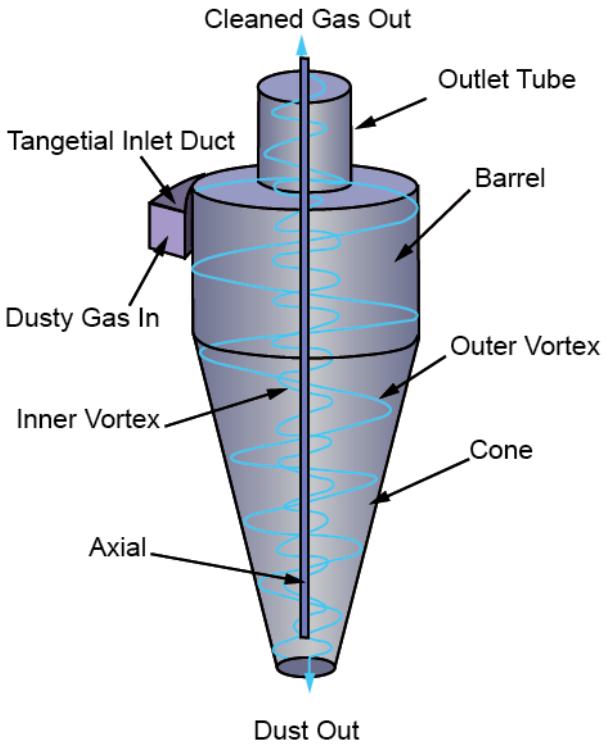

Figure 1.8: Schematic Diagram of reverse flow Cyclone Separator

1.5.2 Uses in different industries

Cyclones are used in various industries where the particulate matter is a vital pollutant. It is generally preferred by these industries as of its low maintenance cost and high efficiency as a controlling device. Following are the few examples where cyclone separators are used:

- At sawmills to isolate the sawdust from the approaching air from cutting process.
- Cyclones are utilized as a part of oil refineries to isolate oils and gases from the polluted air.
- In the cement industries as parts of kiln preheaters.
- Cyclones are logically utilized as a part of the household cleaning units, as bag-less type of compact vacuum cleaners and focal vacuum cleaners.
- Cyclones are likewise utilized as a part of mechanical workshops and kitchen ventilation for removing the oil from the air.
- Smaller cyclones are utilized to isolate airborne particles

1.6 AIM AND OBJECTIVES

The aim of my study is to analyse the changes in pressure drop, velocity profiles and most importantly, the collection efficiency for particulate matter in a cyclone separator by altering the diameter of its exit pipe or vortex finder. The governing equations through the cyclone will be solved by Computational Fluid Dynamics models. The FLUENT module of ANSYS (v18.2) software will be used for solving the CFD equations of the Cyclone.

The objectives of my study will be following:

1. Construction of standard model by referring the S**tandard Stairmand design [4].**
2. Validation of the CFD model created in the present work by comparing the results with that of published literature of **Hoekstra [18]**.
3. To study the various parameters like pressure drop and velocity profiles with variable diameters of vortex finder.
4. Calculation and comparison of collection efficiencies for particulate matter of different geometries of cyclone.

CHAPTER 2

LITERATURE REVIEW

The flow in a cyclone separator has been studied by many researchers but there is no standard model or mathematical equation that can give the exact or pre concluded results. A number of studies and researches are already done for the optimization of the cyclone separator. Many analytical and numerical approaches are used to calculate and predict the flow parameters inside the cyclone.

However, the complexity of the flow inside a cyclone can be predicted by a new set of mathematical equations known as Computational Fluid Dynamics which is reliable and can be solved with more ease as compare to the conventional methods. In this chapter a thorough outline of conclusions and findings are presented after analysing a numbers of research and experiment. My research plan is also given at the end of this chapter after analysing previous studies.

2.1 CYCLONE SEPARATOR AND FLOW CHARACTERSTICS

In reverse-flow cyclone, the swirling motion is made out by designing the inlet section in such a manner that it forces the particle laden gas stream to enter the unit on a tangent to the inner body wall. The inlet is normally of rectangular or circular cross-section. As the gas swirls around, it moves in the downwards in the outer part of the separation space. In the conical part of the cyclone, the gas is slowly forced into the inner region of the cyclone, where the axial movement is upward directed. This flow pattern is often referred to as a **double vortex** (an outer vortex with a downwardly directed axial flow and an inner one with an upwardly directed flow). The gas leaves the cyclone through the **vortex finder**, which is basically a vent pipe for the gas, extends downward from the middle of the roof. This vent pipe has many names, with **vortex tube** and **dip-tube** being the most famous, aside from the vortex finder. The particles in the inlet gas are slung outwards to the wall in the centrifugal field, and are transported to the dust exit by the downwardly directed gas flow near the wall. The most important parameter that affects the cyclone efficiency and flow pattern is the cyclone geometry. For reversed flow cyclones, there are seven geometrical parameters, viz. the inlet height **a**, the inlet

width **b**, the vortex finder diameter $\mathbf{D_x}$, the vortex finder length **S**, the cylindrical part height **h**, the cyclone total height $\mathbf{H_t}$, and the cone-tip diameter $\mathbf{B_c}$. All these dimensions are expressed in terms of barrel or cylindrical part diameter **D** as shown in Fig. 2.1. The two performance indicators used are the **pressure drop** and the **particle collection efficiency**.

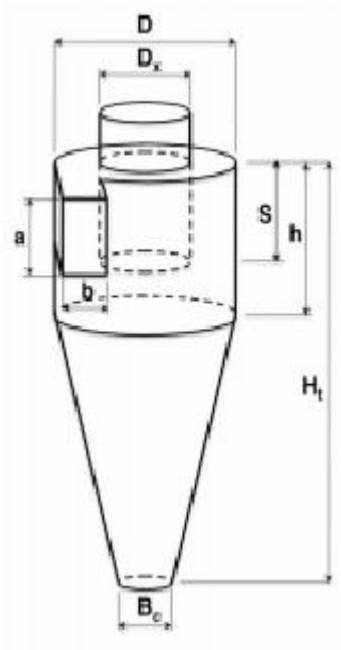

Fig 2.1 Dimension of cyclone separator

2.2 TYPES OF APPROACHES FOR CYCLONE SEPARATOR

There is a widespread literature on the effect of cyclone geometry on performance, using one or more of the four main approaches of study B. Zhao.et al **[7]**, which are:

1) Mathematical models, which can be classified into:
   - theoretical and semi-empirical models
   - statistical models
2) Experimental measurements
3) Computational fluid dynamics (CFD) simulations
4) Artificial neural networks (ANN) approach

2.2.1 Mathematical approaches

First of the theoretical models which were quite significant and well-known were studied by researchers in the mid-20th century (1940-1950). Few of the names are Shepherd and Lapple **[1]**, Alexander **[2]**, First **[3]**, Stairmand **[4]**, Barth **[5]**, Avci and Karagoz **[6]**, Zhao **[7]** and Chen and Shi **[10]**. These models were derived from physical descriptions and mathematical equations which was a complex procedure to follow. A very detailed understanding of gas flow pattern and energy dissipation mechanisms in cyclones is required by these models. In addition, by using different assumptions and simplifying conditions, different theoretical or semi-empirical models can give significant differences between predicted and measured values. Predictions by some models are twice of the experimental values at times as shown by P. K Swamee et al **[11]**.

After the first commercial use of aero-cyclones in 1886 as stated by D. C. Wilcox et al, theories for the valuation of both collection efficiency and pressure drop of cyclone have been developed by many researchers using diverse methods with various simplifying assumptions. Since the past 50 years, the interest in particle collection and pressure drop theories has been steadily increased as examined by B. Zhao and Y. Su. The most common mathematical models for the cut-off diameter and pressure drop calculations are:

- Stairmand model **[4]**
- Shepherd and Lapple model **[1]**
- Casal and Martinez-Bent model **[13]**
- Ramachandran model **[14]**
- Iozia and Leith model **[15]**
- Rietema model **[16]**
- Barth model **[5]**

2.2.2 Experimental methods

A numerous experimental studies have already been performed on the cyclone separators. The most of these studies used either **Particle Image Velocimetry** (PIV) or **Laser Doppler Anemometry** (LDA) to obtain the flow patterns. Some of the studies measured the pressure drop and particle collection efficiency only without any details of

the flow fields. For example, Dirgo and Leith **[17]** measured the collection efficiency and pressure drop for the Stairmand high efficiency cyclone **[4]** only at variable rates of flow. Hoekstra et al. **[18]** measured the mean and fluctuating velocity components for gas cyclones with different geometric swirl numbers by means of the laser doppler anemometry technique. The experimental data from his study clearly shows a strong relationship of the geometric swirl number on the mean flow characteristics, with respect to vortex core size along with the magnitude of the maximum tangential velocity. It is shown that the forced vortex region of the flow is dominated by the so-called precessing vortex core. Hoffmann et al. **[20]** investigated the effect on the separation efficiency and the pressure drop with respect to the cyclone height experimentally and theoretically by varying the barrel length. They analysed the results for cyclone lengths from 2.65 to 6.15 times cyclone diameter (**D**), and found a marked improvement in cyclone performance with increasing length up to 5.5 times of cyclone diameter (**D**). Beyond this length, the separation efficiency has dramatically reduced.

2.2.3 Computational fluid dynamics (CFD)

Boysan et al. **[21]** presented the first CFD investigation in the field of cyclone separators. From that time, the CFD technique becomes a widely used approach for the flow simulation and performance estimation for cyclone separators. For example, Griffiths and Boysan **[21]** computationally investigated three cyclone samplers. They reported that the CFD predicted pressure drops are in excellent agreement with the measured data. The CFD modeling approach is also able to predict the features of the cyclone flow field in great details, which providing a better understanding of the fluid dynamics in cyclone separators **[22]**. Consequently, CFD approach is a reliable and relatively inexpensive method of examining the effects of a number of design changes. Moreover, this makes the CFD methods represent a cost-effective route for geometry optimization in comparison with the experimental approach. Another example, Gimbun et al. [23] successfully applied CFD to predict and to evaluate the effects of temperature and inlet velocity on the pressure drop of gas cyclones [7]. The successful application of CFD technique in different studies in cyclone separators has been reported by many researchers. Nevertheless, CFD is still more expansive in comparison with the mathematical models approach. The main reasons behind the cost of the CFD approach with respect to the mathematical methods are:

1. In essence, the CFD process requires expert intervention by an expert researcher at every stage (mesh generation, solver settings and post processing).

2. The license cost of the grid generator, solver and post processor.

3. The running cost especially for unsteady simulations which need also parallel processing.

4. CFD results always need (i) validation with experimental results (ii) perform the same simulation on different grids to be sure that the obtained results are grid independent.

2.3 THE VORTEX FINDER DIMENSIONS

The vortex finder size is an especially important dimension, which significantly affects the cyclone performance as its size plays a critical role in defining the flow field inside the cyclone, including the pattern of the outer and inner spiral flows. Saltzman and Hochstrasser **[24]** studied the design and performance of miniature cyclones for repairable aerosol sampling, each with a different combination of three cyclone cone lengths and three gas outlet diameters. Iozia and Leith **[15]** optimized the cyclone design parameters, including the gas outlet diameter, to improve the cyclone performance using their optimization program. Kim and Lee **[25]** described how the ratio of the diameters of cyclone body D and the vortex finder Dx affected the collection efficiency and pressure drop of cyclones, and proposed an energy-effective cyclone design. Moore and Mcfarland **[26]** also tested cyclones, with six different vortex finders, and concluded that the variation in the gas outlet diameter under the constraint of a constant cyclone Reynolds number produced a change in the aerodynamic particle cut-off diameter. Recently, Hoekstra **[18]** investigated the effect of gas outlet diameter on the velocity profile using 2-D axisymmetric simulations. Lim et al. **[27]** examined experimentally the effect of the vortex finder shape on the collection efficiency at different flow rates but without any explanation on its effect of the flow field pattern and velocity profiles. Raoufi et al. **[28]** duplicated numerically the same study of Lim et al.

2.5 PREVIOUS OPTIMIZATION STUDIES

Due to the wide range of industrial applications of the cyclone separator, it was a matter of study for decades. However, the optimization studies on it is quite limited in literature. Moreover, many of these studies are not coherent studies. Ravi et al. **[29]** carried out a multi-objective optimization of a set of N identical reverse-flow cyclone separators in parallel by using the non-dominated sorting genetic algorithm (NSGA). Two objective functions were used: the maximization of the overall collection efficiency and the minimization of the pressure drop. Non-dominated Pareto optimal solutions were obtained for an industrial problem in which 165 m^3/s of air was treated. In addition, optimal values of several decision variables, such as the number of cyclones and eight geometrical parameters of the cyclone, are obtained. Their study shows that the barrel diameter, the vortex finder diameter, and the number of cyclones used in parallel, are the important decision variables influencing the optimal solutions. Moreover, their study illustrates the applicability of NSGA in solving multi-objective optimization problems involving gas-solid separations. The main drawbacks of their study are: (1) They used the model of Shepherd and Lapple **[1]** for predicting the dimensionless pressure drop (Euler number). In the Shepherd and Lapple model, the Euler number depends on only three factors ($Eu=16ab/D_x^2$) and they used it to optimize the seven geometrical parameters. (2) The barrel diameter, number of parallel cyclones and the gas velocity have been included into the optimization design space. Consequently, it is not devoted to the geometrical ratio. (3) They usedmany side constraints on the geometrical values ($0.4 \leq a/D \leq S/D$, $0.15 \leq b/D \leq (1 - Dx/D)/2$ if $0.5 \leq Dx/D \leq 0.6$) these constraints prevent searching for the global optimization geometrical ratios for the seven geometrical parameters. (4) No table for the non-dominated Pareto front points are presented from which the designer can select certain geometrical ratio set (optimal solution). Swamee et al. **[11]** investigated the optimum values of the number of cyclones to be used in parallel, the diameter of cyclone barrel D and exit pipe Dx, when a specified flow rate of gas is to be separated from solid particles, and the cut diameter is already specified. They used Stairmand model for calculation of pressure drop and Gerrard and Liddle formula for the cut-off diameter **[11]** which is not a widely used model. Instead of handling two objective functions, they blended the two objective into a single objective problem which is not the suitable method to considering two conflicting objectives (the pressure drop and cut-off

diameter). Safikhani et al. **[30]** performed a multi-objective optimization of cyclone separators. First, they simulated many cyclones to obtain the pressure drop and the cut-off diameter and used artificial neural network approach to obtain the objective function values. Finally, a multi-objective genetic algorithms are used for Pareto based optimization of cyclone separators considering two conflicting objectives. However, the design variables are only four (instead of seven): the barrel height, the cone height, the vortex finder diameter and length. So they ignored the effect of inlet dimensions, which has been acknowledged by other researchers as significant geometrical parameters for the cyclone flow field and performance (cf. Elsayed and Lacor **[33, 34]**). Moreover, they did not explain why they selected these particular parameters. Furthermore, they applied four side constraints on the four tested variables, which prevent searching for the global optimization.

CHAPTER 3

MATERIAL AND METHODOLOGY

3.1 GOVERNING EQUATIONS

The flow in the cyclonic separator is always turbulent in nature and characterized by Reynolds number. Cyclone Reynolds number **Re** is calculated on the basis of cyclone diameter or barrel diameter and flow parameters at inlet, which is given by:

$$\mathbf{Re} = \frac{\boldsymbol{\rho U o D}}{\mu}$$

where **ρ** and **μ** are the densities of gas and viscosity, respectively. **Uo** represents inlet flow velocity and **D** is the diameter of cyclone. Numerical calculations are solved for the gas and solid interactive flow using **CFD approach**. The flow is assumed is assumed to be steady, turbulent, incompressible and isothermal . The gas flow fields are attained by solving together the continuity and the momentum equations. The **Reynolds Stress Model** (RSM) is used to represent the turbulent flow and the **Discrete Phase Model** (DPM) is used to forecast particle trajectories and collection efficiency. The particle equations of motion are solved to track the particles trajectories in the flow field and also the relevant forces acting on each particle are taking into account. The 3-D gas and particle interactive flow in cyclone separators is defined by the assumption that the particulate phase is in dilute state and particle loading rate is low as compared to the air flow. That is why, the interaction between particles and flow is kind of negligible. Plus, the particles do not distress the gas flow field through the flow. So the case in the study is computed using an assumption of **one-way coupling** in the cyclone separator. The contributing terms in the Navier-Stokes equations due to gas-solid momentum exchange are neglected due to this assumption.

3.1.1 Transport equations

Singer **[35]** has given the 3-D mass conservation time-averaged equations for turbulent and incompressible behaviour flow and neglected the other forces developed by body:

$$\frac{\partial \overline{u_i}}{\partial x_j} = 0,$$

$$\rho \overline{u_j} \frac{\partial \overline{u_i}}{\partial x_j} = -\frac{\partial \overline{P}}{\partial x_i} + \frac{\partial}{\partial x_j}\left[\mu\left(\frac{\partial \overline{u_i}}{\partial x_j} + \frac{\partial \overline{u_j}}{\partial x_i}\right)\right] + \frac{\partial \tau_{ij}}{\partial x_j},$$

Where $\bar{u}_i$ and $\bar{u}_j$ the mean velocities in i and j direction, respectively. x_j is the position, mean pressure is P , τ_{ij} is called Reynolds stresses and it is given by:

$$\tau_{ij} = -\rho u_1' u'$$

The CFD numerical prediction's success rate intensely hinge on the accurate description of turbulent behaviour. Recent studies on numerical models of cyclones separators have shown that selection of turbulence model has substantial effect on the flow field pattern in cyclone separators. Studies have also suggested that the Reynolds Stress Model (RSM) can be responsible for the high unsteady swirl in cyclone separators.

RSM solves the transportation equation for each term of Reynolds stress tensor without the necessity of isotropic turbulent viscosity field. For steady and incompressible flows, RSM is given by the following equation:

$$u_k \frac{\partial}{\partial x} k(\overrightarrow{u_1' u'}) = Dij + Pij + \phi ij - \epsilon ij$$

D_{ij} acknowledges the diffusive transport term which is as follows:

$$D_{ij} = -\frac{\partial}{\partial x_k}\left(\frac{\mu_t}{\sigma_k}\frac{\partial \overline{u_1' u'}}{\partial x_k}\right).$$

P_{ij}, represents the stress is calculated as:

$$P_{ij} = -\rho\left(\overline{u_i' u_k'}\frac{\partial u_j}{\partial x_k} + \overline{u' u_k'}\frac{\partial u_i}{\partial x_k}\right).$$

ϕ_{ij} is the pressure strain

$$\phi_{ij} = \overline{P\left(\frac{\partial u_l'}{\partial x} + \frac{\partial u'}{\partial x_l}\right)}.$$

The dissipative ϵ_{ij}

$$\epsilon_{ij} = 2\mu \overline{\frac{\partial u_i'}{\partial x_k} \frac{\partial u'}{\partial x_k}}.$$

Launder and Spalding [36] has given the near wall function. The law of the wall for mean velocity is given by:

$$\frac{U C_\mu^{1/4} k^{1/2}}{\tau_w / \rho} = \frac{1}{\kappa} \ln\left(E \frac{\rho C_\mu^{1/4} k^{1/2} y}{\mu} \right)$$

In the above equation, Von Karman constant is **κ**. $\mathbf{C_\mu}$, **E** is the empirical constants whereas, μ is the fluid viscosity. The fluid velocity, turbulent kinetic energy and normal distance to the wall at the point is *U, k, y* , respectively. τ_w is the wall shear stress.

3.1.2. Discrete Phase Model (DPM)

The discrete phase model is employed to calculate particle trajectories in the flow and to track every particle through the volume of fluid. It is based on the Lagrangian approach. In Cartesian coordinates, the equation of motion for any particle in the control volume is as follows:

$$\frac{d\vec{U}_p}{dt} = \frac{18\mu}{\rho_p d_p^2} \frac{C_D \mathrm{Re}_p}{24} (\vec{U} - \vec{U}_p) + \frac{\vec{g}(\rho_p - \rho)}{\rho_p}$$

Here, the fluid and particle velocity vectors are $\bar{\mathbf{U}}_\mathbf{p}$ and $\bar{\mathbf{U}}$, respectively. Fluid and particle densities are represented by **ρ** and $\boldsymbol{\rho}_\mathbf{p}$ and **dp** is the particle diameter, C_D represents drag coefficient and the acceleration of gravity vector is **g**. $\mathbf{R_{ep}}$ is the particle relative Reynolds number which can be defined as:

$$\mathrm{Re}_p = \frac{\rho d_p |\vec{U}_p - \vec{U}|}{\mu}$$

At the point when a particle contacts the wall of the cyclone, it bounce back and loses some quantity of its kinetic energy. The proportion of particle rebound velocity and particle impact velocity is known as the coefficient of restitution. The estimations in this

examination are performed utilizing a diverse coefficients of restitution 'e' in the scope of 0.6 to 1 which demonstrated that collection efficiency has not an indispensable association with it. In this way, the computations are done in this investigation by taking a presumption of elastic collisions of particles and wall with coefficient of restitution 'e' being 1 through. Stochastic method is utilized to represent to the impact of turbulent collision on the particle trajectory. In this technique the instantaneous stream velocity is considered as the entirety of the normal velocity and the fluctuating velocity which was figured from the stream turbulent kinetic energy

3.2 PROBLEM DESCRIPTION

S**tandard Stairmand design [4]** is the standard geometry which is used in this study with similar cyclone geometrical parameters. Similar geometry is referred by various researchers. For example, Hoekstra **[18]** used standard stairmand cyclone design and investigated various flow parameters using LDA technique. Three geometries are generated in this study using different diameters of the vortex finder which is given in the Table 3.1. These geometries have different diameters of the vortex finder i.e., 0.4D, 0.5D and 0.6D. CFD terminology is used to forecast the flow field and pressure drop through the cyclone. The tangential and axial velocities are obtained from the flow simulation for the standard Stairmand design and then compared to the existing experimental data of Hoekstra. The results obtained from the standard Stairmand design are then subjected to the optimization. Dimensional analysis is been done to find out the cyclone performance using dimensionless quantities.

Part Name	Dimensions
Cyclone diameter, D	290 mm
Inlet height, a	0.5 D
Inlet width, b	0.2 D
Cone-tip diameter, Dc	0.37 D
Exit pipe diameter, Dx	0.6 D, 0.5 D(**Standard**), 0.4 D
Cylindrical part height, h	1.5 D
Cone part height, hc	2.5 D

Length of inlet section, Li	1.38 D
Length of cylindrical barrel top, Le	D
Exit pipe length, S	0.5 D

Table 1: Dimensions of the tested Cyclone Separator model

In this study, a standard cyclone geometry based on Stairmand design is first designed in the computer and simulated in **Ansys Fluent 18.2**. The obtained data for standard cyclone is then compared with the work of Hosketra to validate the model. A grid is

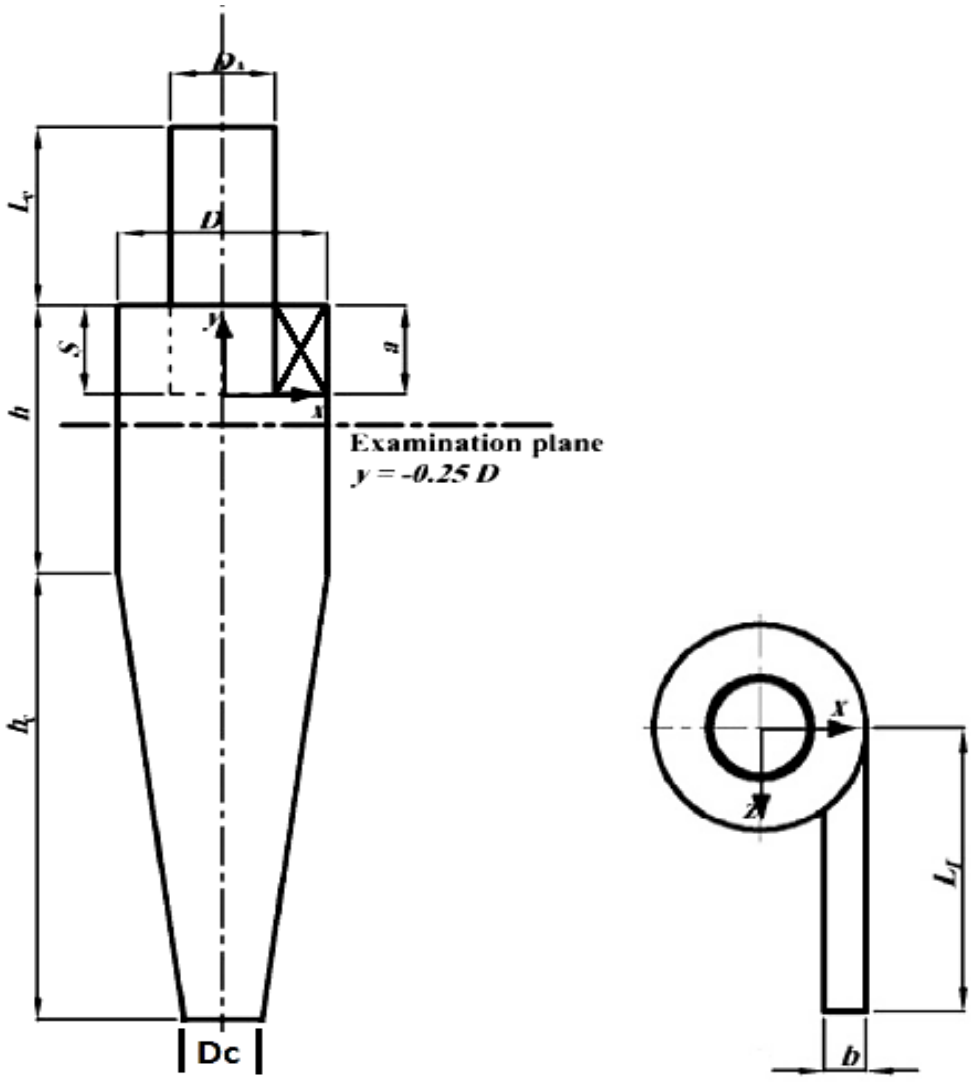

Figure 3.1 Schematic diagram of Standard Cyclone Geometry. Front and top views

generated of specific cells and nodes for the computation. The description about the grid is given further in this chapter.

In this study of cyclone separator, only the effect of different vortex finder diameters are taken into account so all the other dimensions will remain constant. Only vortex finder diameter i.e., $\mathbf{D_x}$ will vary in all the designs. The objective will be to study the effects on the pressure drop, velocity profiles and collection efficiency of particulate matter with rendering the D_x. For all the evaluation and calculation, a reference section is considered at -0.25 D from the origin to compare the results obtained as shown in Figure 3.1.

3.2.1 Grid generation

A computational grid is constructed using 3-D blocks unstructured method. The grid or mesh is generated using meshing module of **Ansys Workbench** called **ICEM**. Due to the complicated geometry of cyclones, **Hexahedral meshing** is employed which is a collection of cubes. Hex meshing is the most complex meshing to create numerical grid blocks but on the other hand it is the most accurate for complicated geometries like cyclone separator.

There are total 35 blocks with in the geometry due to complicated design of the cyclone separator. Total 3 O-grids are created of the main central block and then split over each face to properly overlap the whole cyclone body. Each block is then associated with the faces of geometry. The meshing details are in Table 3.2 for the standard geometry.

The grid is constructed in such a way that the 2-D computational grid will overlap the cyclone cross-section with quad elements all around. Then the cross-sectional grid is derived through the whole cyclone length to form a 3-D mesh or a grid with hexahedral elements. The numerical mesh is being thick in the boundary layer and in sections of high velocity gradients that is vital to accurately predict flow behaviour in these regions. Three numerical mesh or grids are produced for the three geometries considered in this study. The numerical grid for the standard Stairmand geometry is as shown in the Figure 3.2.

Element	Number
Nodes	**579379**
Quads	**28846**
Hexas	**565404**

Table 3.2: Grid details of standard cyclone geometry

As showed in the table, the standard design consists of 579379 nodes, 28846 quads and 565404 hexas. The grid dependency studies are carried out further in the chapter. The above grid details are for 0.5 D geometry which is considered as standard geometry in this subject. Different grids with varying elements are tested for each geometry. The main concern is about the exit pipe diameter. To generate a mesh on the vortex finder, the face of blocks for vortex finder is copied with the surface grid which got overlapped perfectly to the vortex finder. Same is shown in Figure 3.3. Same is also done for the exit pipe length and inlet duct. A dense meshing also known as inflation layers of mesh is installed at the boundaries of the geometry to accurately calculate the parameters during the simulation. Denser mesh has more cells or elements which will help in solving the flow equations more precisely thorough them. Inflation layers are installed manually by altering the mesh settings and visualising an appropriate grid which will perfectly sums up with the cyclone geometry.

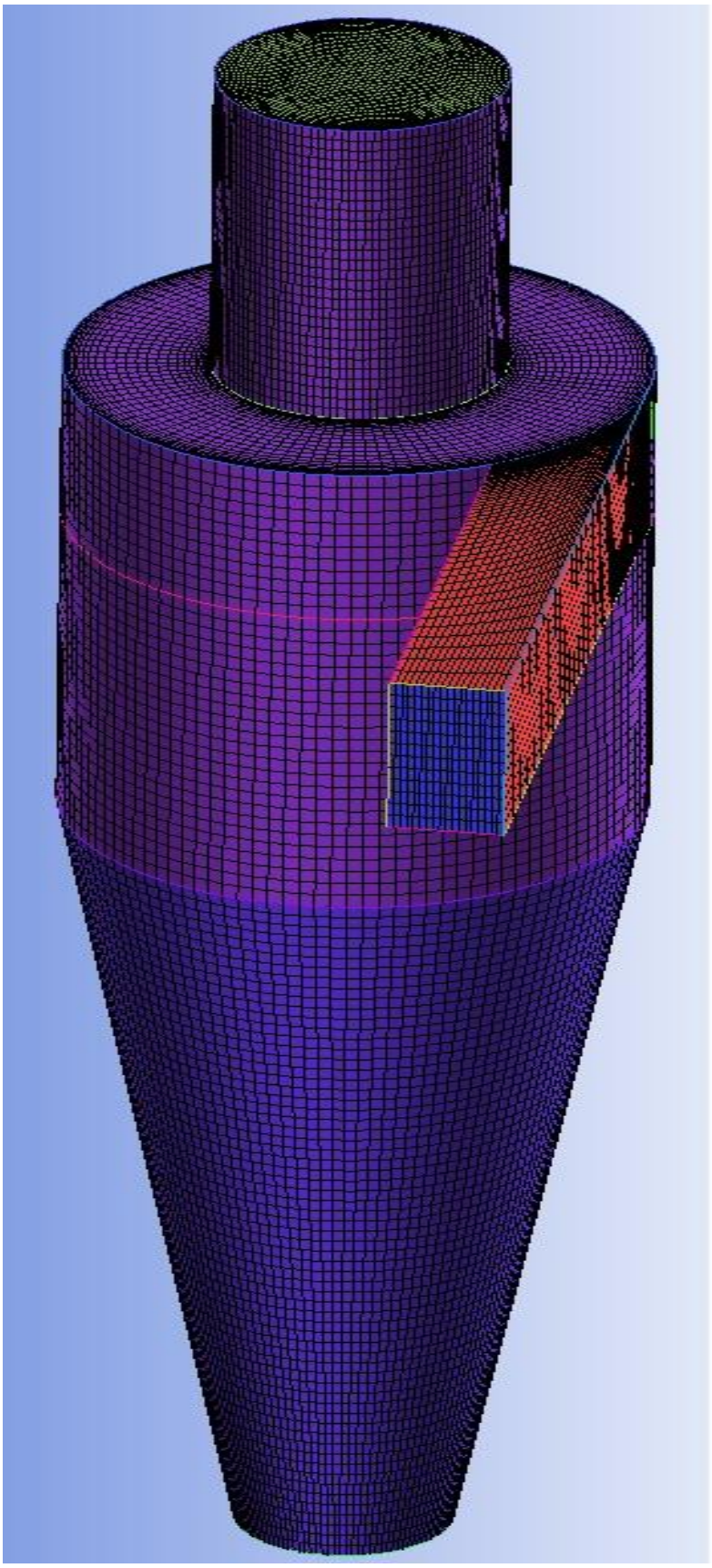

Figure 3.2: Generated grid of standard Cyclone Geometry

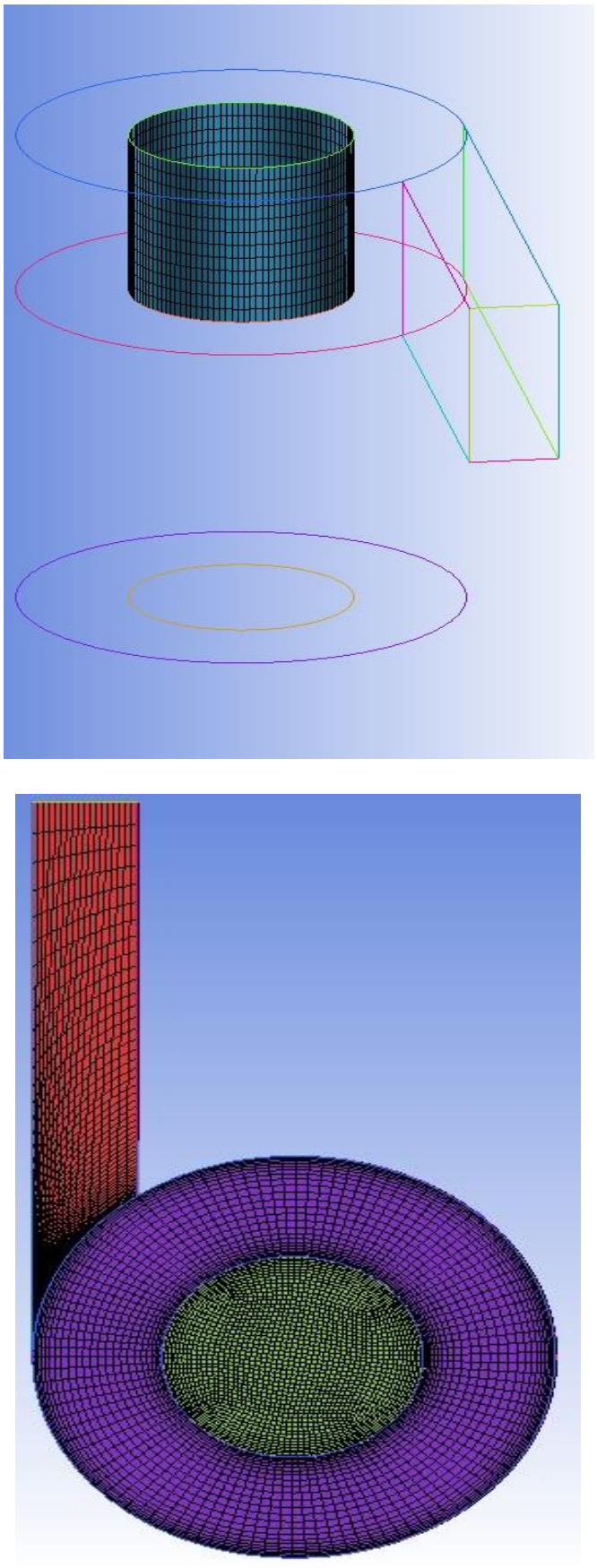

Figure 3.4: Pictures of generated grid at vortex finder and inflation layers at boundary

3.2.2 Boundary conditions

The boundary conditions at inlet are assigned from the data of Hoekstra **[18]** experimental analysis. The flow is simulated in different cyclone designs at inlet velocities of 5, 10, 15, 20, 25 and 30 m/s. Velocity distribution is considered as uniform.

The inlet and both outlets are considered as pressure inlet and outlet. Turbulence intensity is taken as 5% at inlet and 0% at both the outlets. Hydraulic diameter at inlet is 0.145 m. Hydraulic Diameter of exit pipe (vortex finder) is different for different diameters. For standard geometry, it is taken as 0.145 m and 0.1073 at trap bin outlet. The assumption of fully developed flow is considered at the outlet. No-slip boundary condition was used at all walls. Radial equilibrium pressure distribution is considered at both the outlets.

3.2.3 Solver Settings

The CFD code FLUENT of Ansys Inc. is used to solve the time-averaged equations of the gas flow. CFD code FLUENT is based on a finite volume discretization method on unstructured numerical mesh. SIMPLE (Semi-Implicit Method for Pressure-Linked Equations) is the finite volume solution approach which is used in this study for velocity and pressure coupling. To interpolate the parameters on the surface of the control volume, second order upwind schemes are used. Iterative approach is used to solve the time averaged equations. The solution is considered to be converged when the normalized error reached $\mathbf{1 \times 10^{-5}}$. The calculations were performed on a CPU consisting of dual core i3 6^{th} generation processors (2.00 GHz and 1.99 GHz) with 4 GB of RAM.

3.2.4 Solution grid dependency study

The response of the numerical simulation to the grid sizing and elements are tested for standard Stairmand geometry. Two types of computational meshes are used with elements around 580000 and around 370000 cells. The obtained pressure drops using these grids are then tested against different velocities, which is shown in Table 3.3. The maximum difference between the investigated results obtained by using coarse and the fine meshing is less than ±0.4% which is clearly proved by the table. That is why, the

finer grid with 580000 cells is the assigned grid which is used in all calculations of standard geometry. This grid dependency study is carried out to be sure that the obtained results are grid independent. The hexahedral computational grids were generated using Ansys ICEM 18.2 mesh generator and the simulations is carried out in Ansys Fluent 18.2

Inlet velocity (m/s)	Pressure drop (Pa)		Error (%)
	580000 cells (Finer Grid)	**370000 cells (Coarse Grid)**	
15	542.66	541.82	0.155 %
20	970.5	969.75	0.103 %
25	1535.74	1537.63	-0.123 %
30	2205.74	2214.33	-0.389 %

Table 3.3.: Gird dependency study results

3.3 GEOMETRICAL AND GRID DETAILS OF THE TESTED CYCLONES

(A) (B) (C)

Figure 3.5: Picture of three cyclone models which are tested with different vortex finder diameter

In the above discussion about the study, the details about the standard geometry have already been stated with the grid details. It is also important to give a broader view about all the other tested geometries which is used to calculate results. There are total 3 geometries including the standard one with the only difference of varying diameters of vortex finder and all the dimensional parameters remains constant through the study. A better view of this can be taken from the Figure 3.5 which describes all the three geometries with their respected vortex finder diameters. The part (B) is the standard Stairmend geometry of cyclone separator with D_x=0.5 D. (A) and (C) are tested to study the comparison and dependency of velocity, pressure drop and collection efficiency on vortex finder. Geometry (A) being with smaller dia. of exit pipe and geometry (B) with bigger dia. of exit pipe. The grid details are given in Table 3.4.

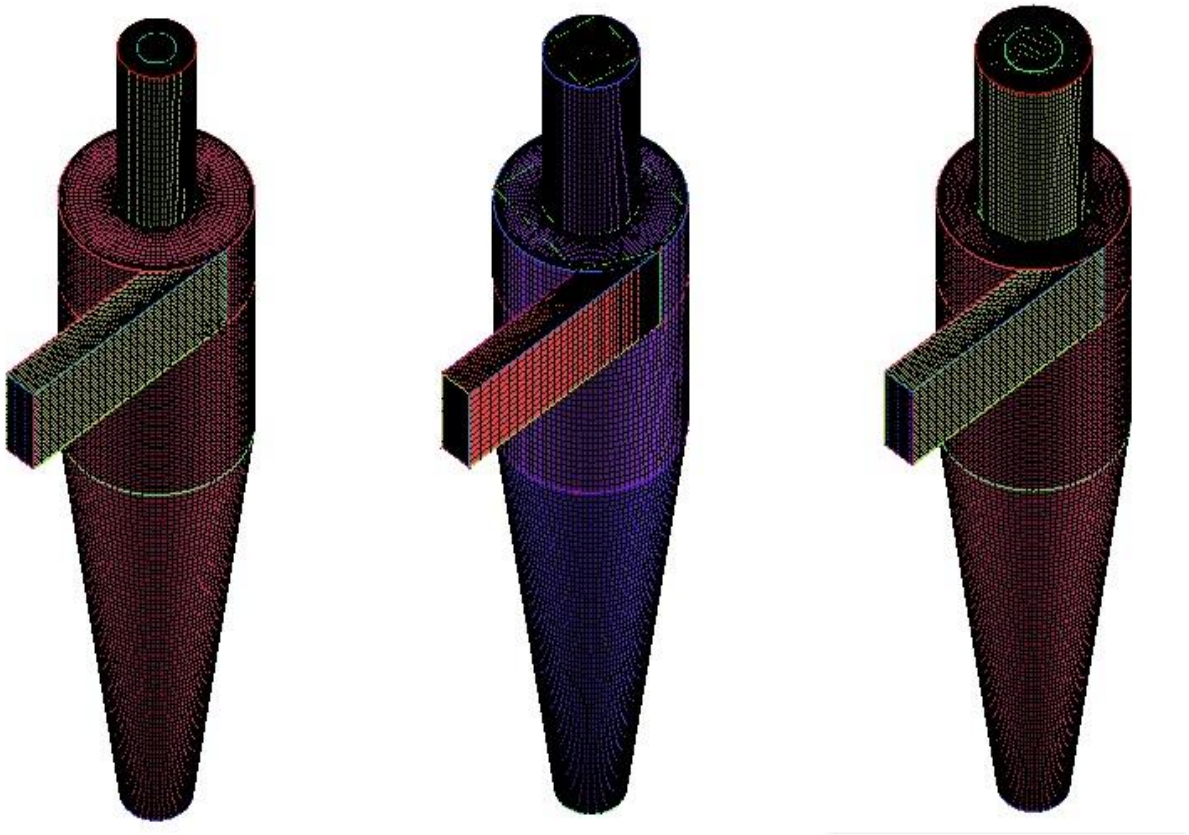

(A) (B) (C)

Figure 3.6: Picture explaining the detailed grid generated for all the three tested cyclone models

Above figure explains the hex meshing which is used as a grid for the cyclone geometries. Hex meshing is generated in meshing code ICEM of Ansys (v18.2) which is quite reliable for computational analysis of complex shapes. The details about grids can be seen in Table 3.4.

0.4 D geometry		**0.5 D geometry**		**0.6 D geometry**	
Element	**Value**	**Element**	**Value**	**Element**	**Value**
Nodes	617620	Nodes	579379	Nodes	783465
Quads	28032	Quads	28846	Quads	30432
Hexs	604512	Hexs	565404	Hexs	769152

Table 3.4: Grid details of all the generated geometries

CHAPTER 4

RESULTS AND DISCUSSIONS

In all the previous researches and studies, it has been found out that the vortex finder dimension causes a significant effect on the cyclone performance and flow pattern. But the previous studies are not comprehensive and did not present vital details about the effect of geometrical parameters on the pressure drop and the collection efficiency of particulate matter. Also the detailed evaluation about the effect of the vortex finder dimension on various types of velocities i.e., **tangential** and **axial** velocity, is rare to find in the old literature. The present study is intended to computationally solve the flow equations through the cyclone to study the effect of increasing the exit pipe diameter $\mathbf{D_x}$ on the pressure drop and collection efficiency for particulate matter and to gain more details about the flow pattern and velocity profiles using the Reynolds Stress Model (RSM) methodology.

4.1 MODEL VALIDATION

Model validation is an important step to perform while analysing a model computationally. It gives a freedom of changing certain physical parameters after the basic model has been verified with the previous work. A slight error can be neglected as far as it follows the expected trends and behaviour. In this study, the model validation is done on the reference geometry and its three types of velocity profiles and pressure drop is calculated and confirmed by comparing with the past calculation done by researchers.

The flow field is computed by comparing the results obtained for velocity profiles in the cyclone with the experimental results obtained by of Hoekstra **[18]** for the standard Stairmand design using LDA technique. The profiles of tangential and axial velocities are examined at an axial position of **y = 0.25 D** below the vortex finder. The origin of the model is where the cover plate of vortex finder starts as displayed in Figure 3.1 in the previous chapter. The position of y= 0.25D is said to be the examination plane for this study. The flow is analysed for incoming velocity of $\mathbf{U_o=15}$ m/s corresponding to Reynolds number of cyclone Re = 2.8×10^5.

The comparison of numerical obtained results in the present study and the experimental results of the published literature for axial and tangential velocity profiles are shown in figure 4.1 and figure 4.2. The velocities are shown as dimensionless using the ratio of instantaneous velocity at a point to incoming velocity $\mathbf{U/U_0}$. The figures show that the calculated velocity profiles matches appropriately with the experimental values. The axial velocity profile indicates that the gas flow is downward near cyclone wall and upward near cyclone core which basically predicts the pattern of separation process that happens in the cyclone. It can be stated by evaluating the profiles that the downward velocity near the wall is responsible for particle separation, not the gravity. When the particle is subjected to the centrifugal force, they start moving in downward direction and then collected in cyclone dust collector or outlet 2 in this geometry.

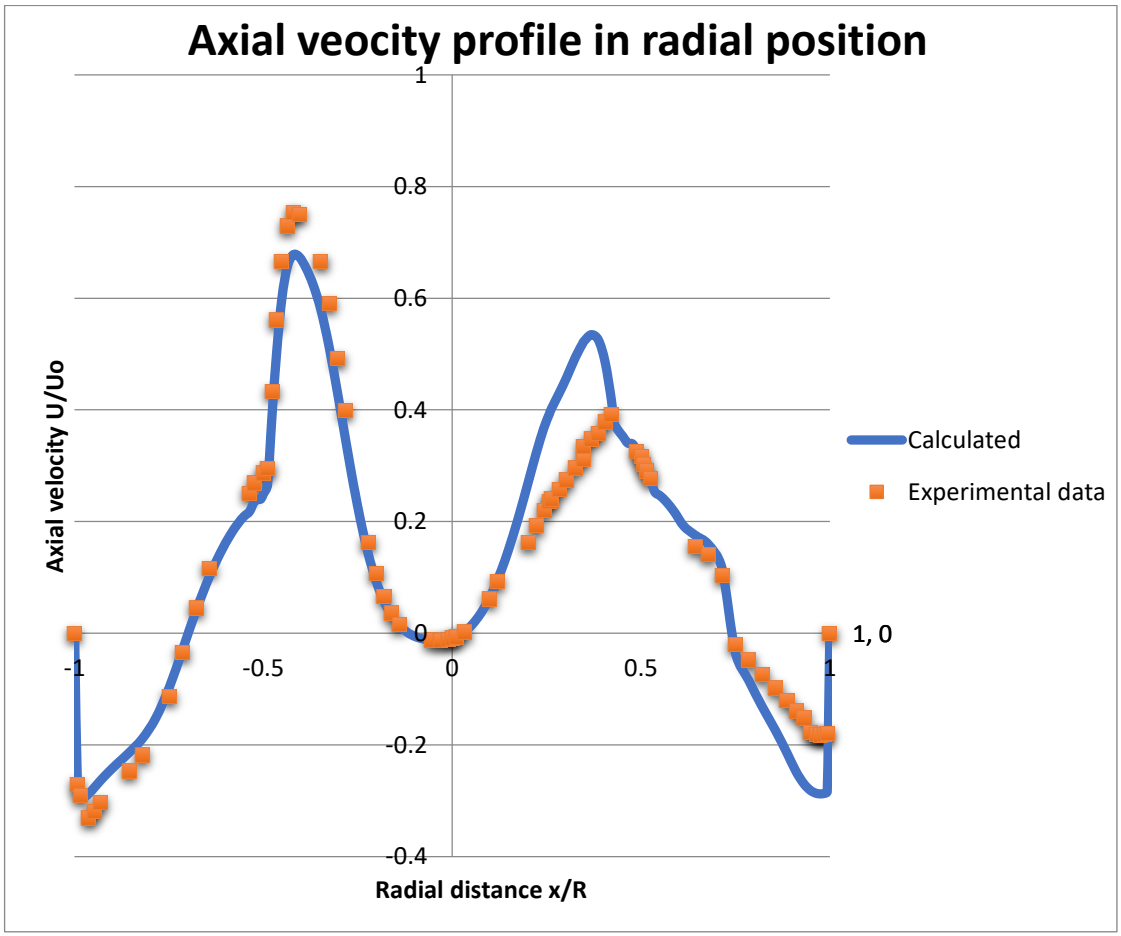

Figure 4.1: Graph showing variation of dimensionless axial velocity vs radial position for calculated results and experimental data of *Hoekstra* at axial position of y =0.25D

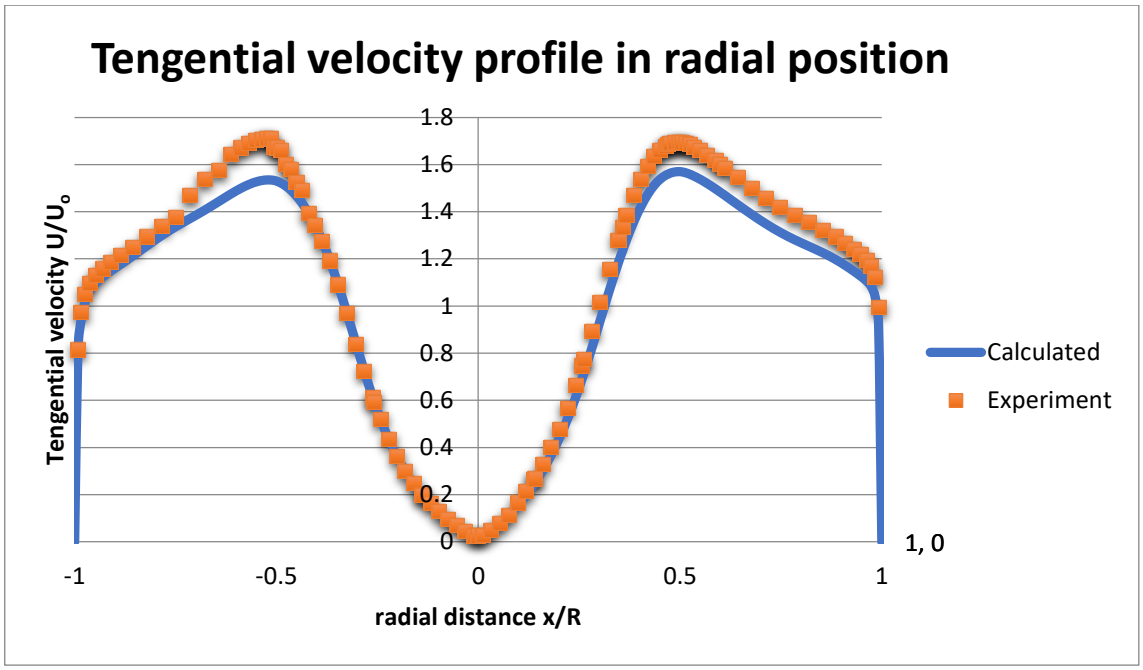

Figure 4.2: Graph showing tangential velocity profile with comparison of calculated and experimental data at y=0.25 D

4.2 AXIAL VELOCITY

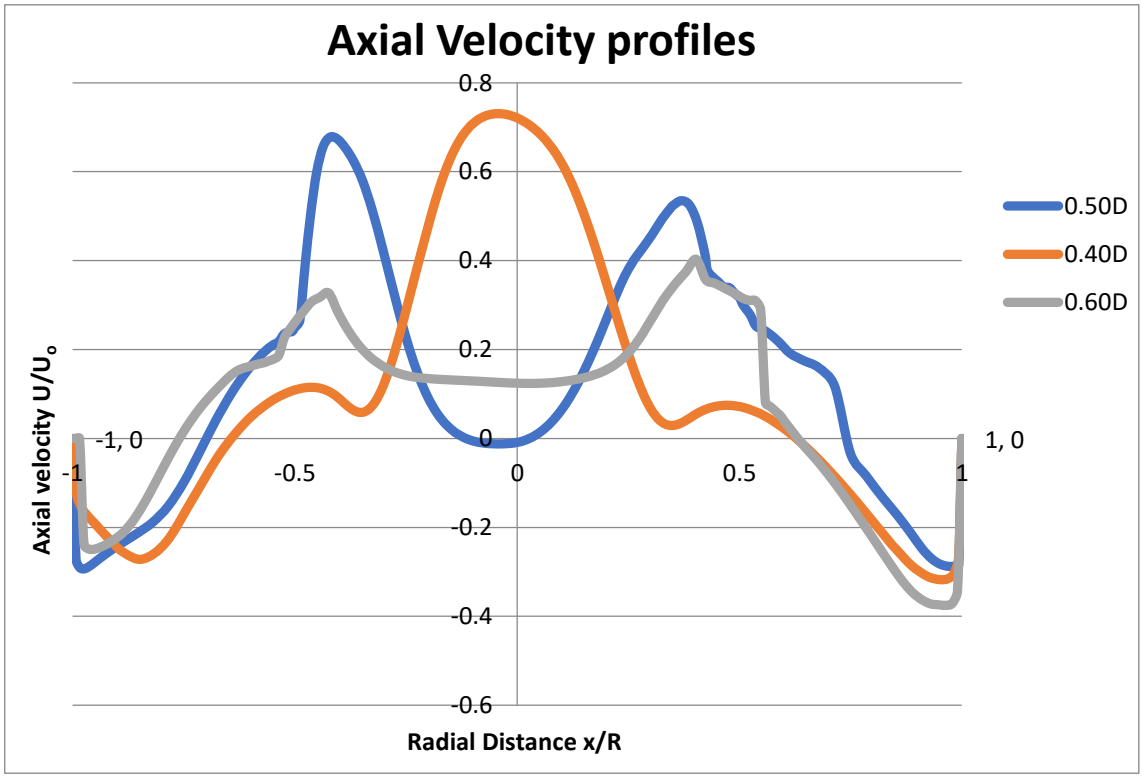

Figure 4.3: Graph showing variation of axial profile comparison of all the three models together in radial direction at y= 0.25D

From Figure 4.3, the evaluation of dimensionless axial velocity profiles through cyclone model can be done. The variation profile is given at the axial position of y =0.25D and for the inlet velocity of 15 m/s. The profile shows inconsistencies from the axisymmetric profiles. This is due to the close location observation plane from the inlet.

Figure 4.3 indicates that with decreasing of vortex finder diameter, an increase of upward axial velocity occurs in the cyclone. The axial velocity profile changes from the inverted W to the inverted V profile as the vortex diameter decreases. This phenomenon occurs in the cyclone for adjusting the decrease in diameter of vortex finder. The graph also indicates that for the larger vortex finder diameter, two peaks are obtained in the axial profile. The spike in the velocity increases with decreasing the diameter of vortex finder. Also, the gap in between these high peak values diminish and the maximum velocities unites together into one large peak eventually for lesser vortex finder diameter that can be seen in $D_x = 0.4D$.

In figure 4.4, contours of axial velocity can be seen where it is clear that with the increase of vortex finder diameter, the axial velocity decreases thorough the cyclone. Whereas, with the decrease in the diameter the axial velocity increases.

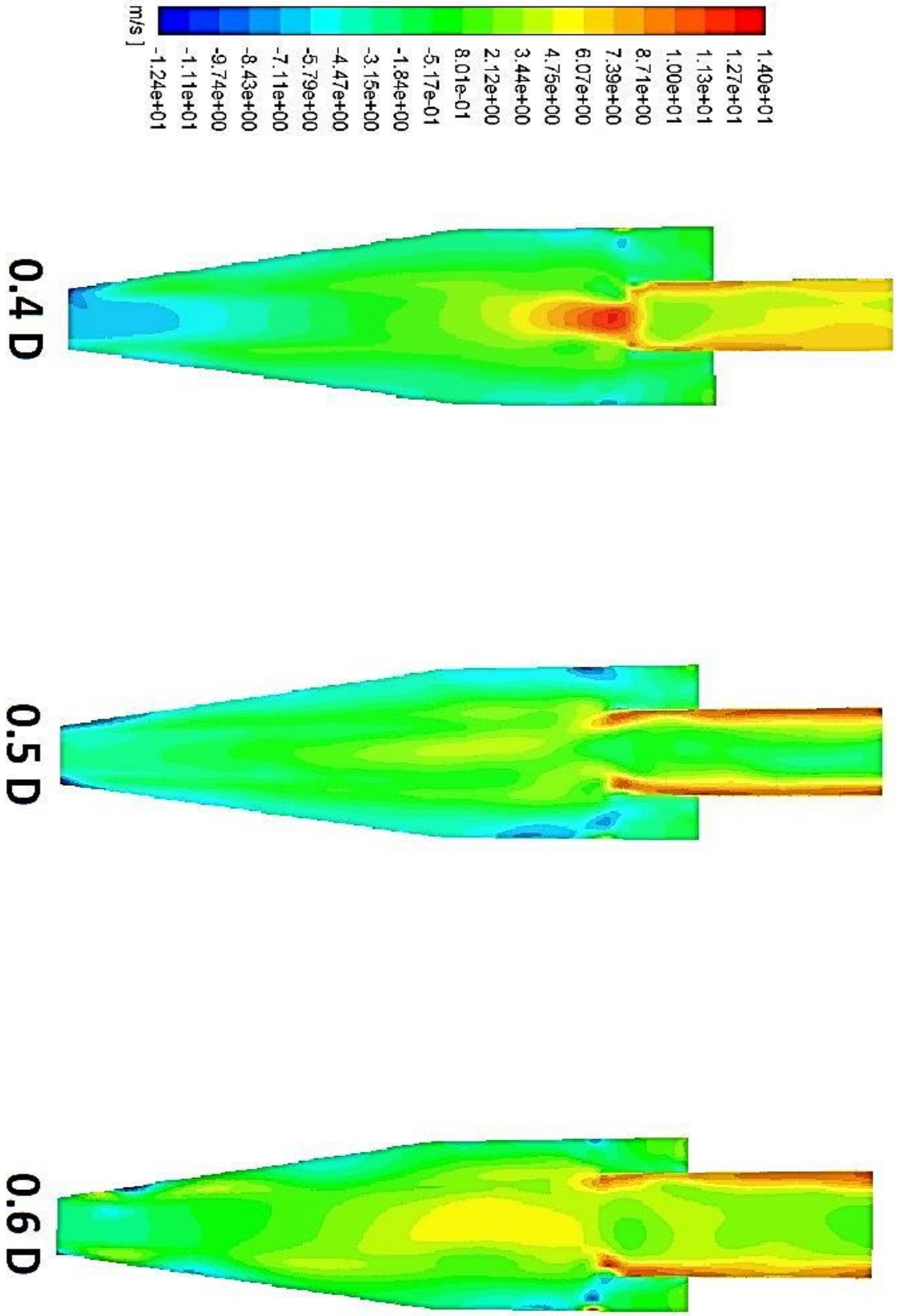

Figure 4.4: Contours of axial velocity of tested geometries

4.3 TANGENTIAL VELOCITY

Tangential velocity has an important role in vortex generation inside the cyclone. Higher values of tangential velocity are responsible for higher swirl speed generation which ultimately increases the collection efficiency of cyclone. In this study, it is found out that the vortex finder diameter influence significantly in tangential velocity generation. The vortex finder diameter is inversely proportional to the maximum tangential velocity attained in the cyclone. Tangential velocity is always zero at the center of the cyclone and increases progressively as moving away from the mid plane.

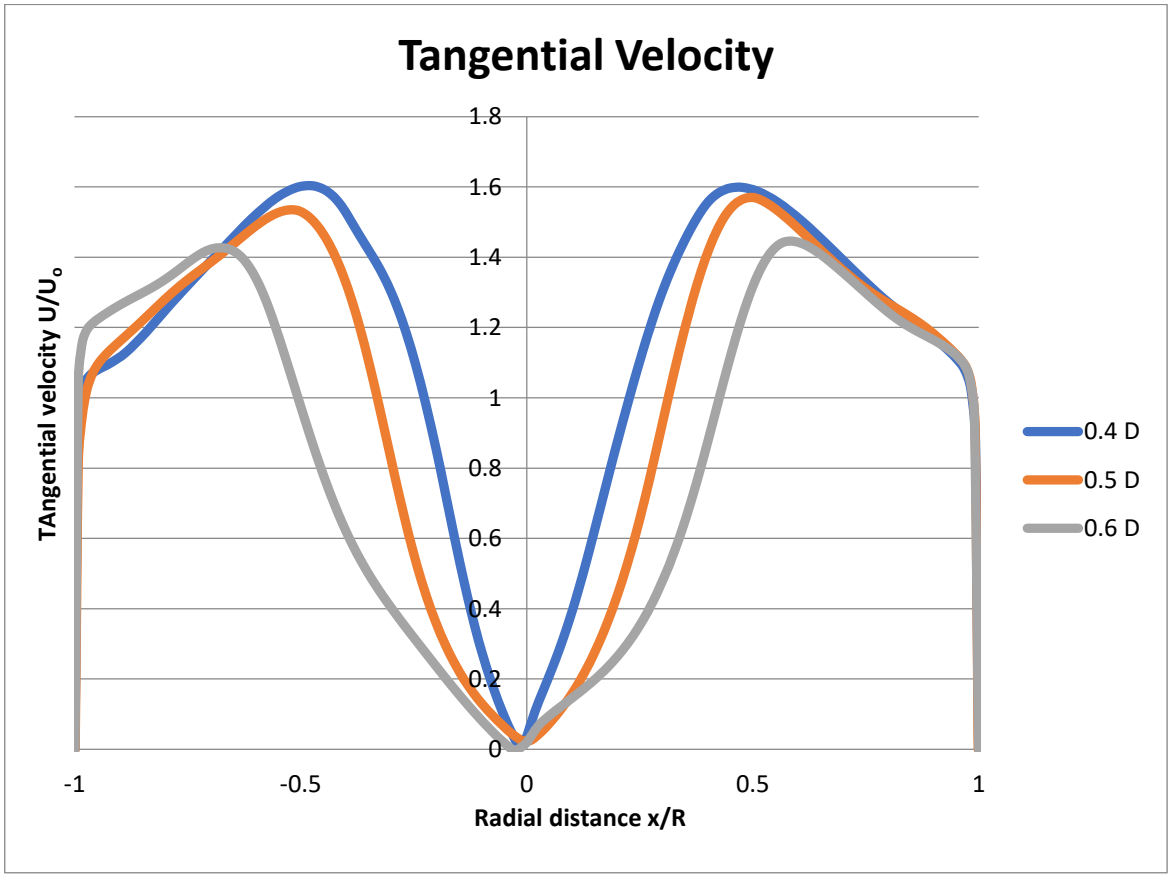

Figure 4.5: Tangential velocity gradients at y =0.25D for different vortex finder diameter

The tangential velocity graphs using different diameters of vortex finder can be seen in figure 4.5. This velocity is taken at the axial position of y =0.25D. The Inlet velocity is same as for obtaining axial velocity variation i.e., U_o = 15 m/s^2. The graph shows that high value of maximum tangential velocity is gained using smaller diameter. The dimensionless tangential velocity contours is shown in figure 4.6 which also indicate that by decreasing vortex finder diameter, an increases in tangential velocity occurs.

Whereas, larger the diameter of vortex finder, lesser is maximum the tangential velocity attained in the cyclone. It can give a clearer view as far as the efficiency is concerned. 0.4 D geometry attains maximum tangential velocity so it is more efficient in terms of swirling speed.

Tangential velocity contours also shows the same variation of velocity attainment. Much darker red contours which show the higher values of speed are more in 0.4 D and 0.5 D geometry. Light speed contours can be seen in 0.6 D geometry.

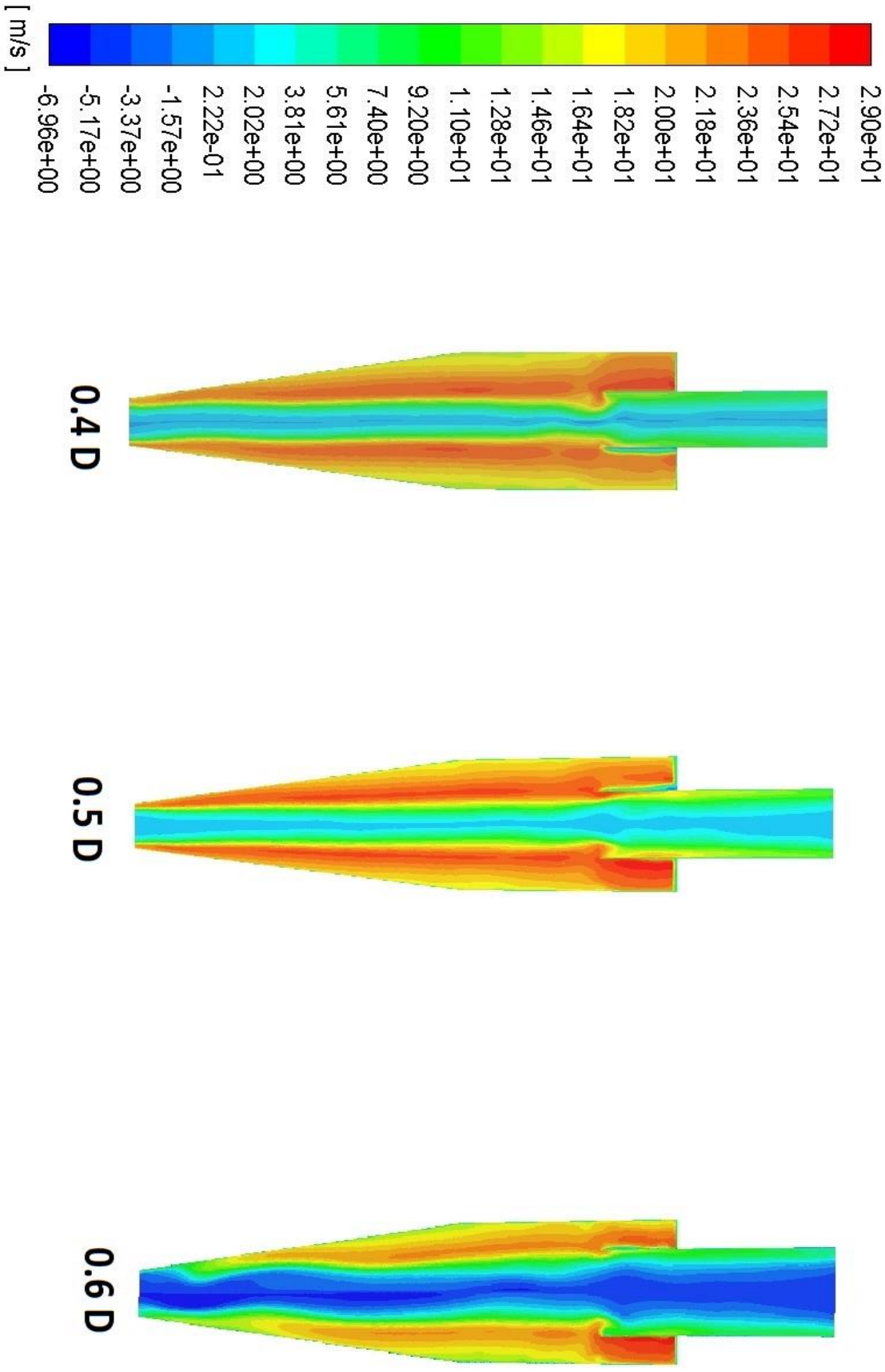

Figure 4.6: Tangential velocity contours of tested geometries

4.4 PRESSURE DROP

Pressure drop across the cyclone plays a significant role in its overall performance. The total pressure drop in a cyclone is due to:

- The entry and exit loss
- Friction loss
- Kinetic energy loss

Kinetic energy loss due to swirl and energy dissipation is the most significant reason of pressure drop. Many attempts have been done by the previous researchers to predict pressure drops from the given design variables. Motivation behind the equation is that one can optimize the design of required cyclones by working backwards. Stairmand **[1]** has given an empirical equation to predict the pressure drop in cyclone.

$$\Delta P = \frac{\rho f}{203}\left\{u_1{}^2\left[1+2\phi^2\left(\frac{2r_t}{r\in}\right)\right]+2u_2^2\right\}$$

ΔP = pressure drop

$\mathbf{u_1}$ = inlet duct velocity

$\mathbf{u_2}$ = exit duct velocity

$\boldsymbol{\rho_f}$ = gas density

$\boldsymbol{\Phi}$ = cyclone pressure drop factor

$\mathbf{A_s}$ = surface area of cyclone exposed to the spinning fluid for design purposes this can be taken as equal to the surface area of a cylinder

$\mathbf{A_t}$ = area of inlet duct

$\mathbf{r_t}$ = radius of circle

$\mathbf{r_\epsilon}$ = radius of exit pipe

$\boldsymbol{\Psi} = f_c\,(A_s/A_1)$

$\mathbf{f_c}$ = friction factor

In this study, CFD methodology is used to compute the pressure drop. Two types of pressure is measured through the cyclone:

1. Static Pressure
2. Total pressure drop

Both the pressure parameters are evaluated for all the three geometries. Graphs and contours are obtained and compared to study the effect of vortex finder diameter on pressure drop.

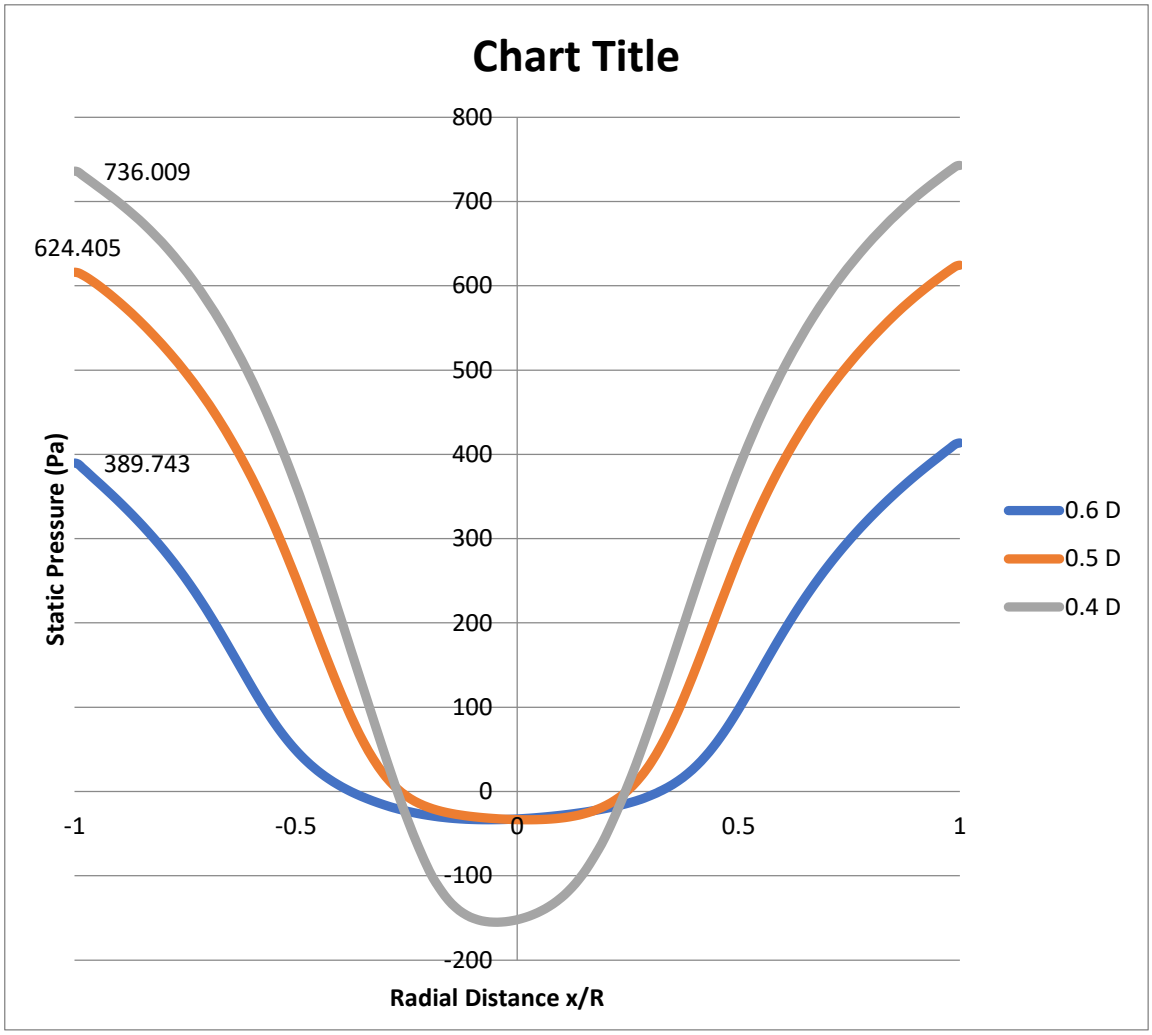

Figure 4.7: Graph of static pressure for all the three geometries at y=0.25D

4.4.1 Static Pressure

Figure 4.7 shows a graph of static pressure variation at axial position of y= 0.25 D for all the three geometries. It can be easily observed that the geometry with vortex finder diameter of 0.4 D shows the highest value of static pressure drop with 736.003 Pa near the cyclone wall whereas the geometry with vortex finder diameter of 0.6 D shows the least pressure drop near the wall with the value of 389.743 Pa. Also the 0.4 D geometry also has the highest negative static pressure at the centre with the value of -154.989 Pa. The geometry of 0.5 D and 0.6 D shows almost equal negative static pressure value of -33.50 Pa and -33.42 Pa respectively.

This clarifies the fact that with increasing the vortex finder diameter, a sharp decrease in the pressure drop occurs. On the other hand, with decreasing its diameter, pressure drop increases significantly. The energy loss in the vortex finder tube is the main contributor to the overall pressure drop in the cyclone, which mainly depends on the maximum tangential velocity in the cyclone. It can be observed in figure 4.5 and 4.6, the maximum tangential velocity decreases with increasing the vortex finder diameter. Contours of static pressure are shown in Figure 4.8.

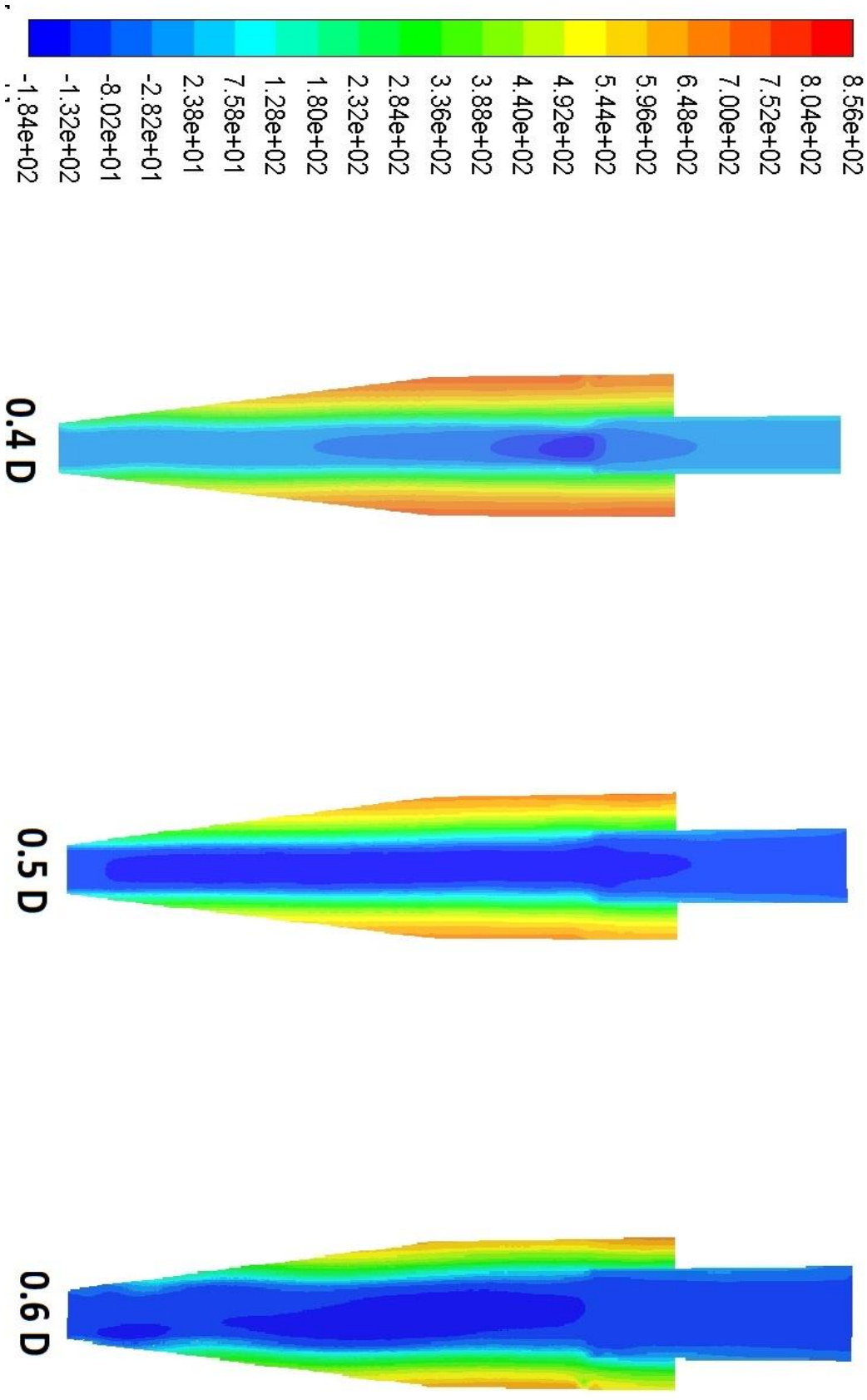

Figure 4.8: Contours of static pressure in cyclone geometries

4.4.2 Total Pressure

Total Pressure is combined term which can be used to represent the overall pressure drop inside the cyclone. Every parameter including static and dynamic pressure drops are included in this term. Total pressure gives more vivid scenario about the pressure filed changes through the cyclone. Total pressure accommodates all type of losses occurs in the cyclone.

Figure 4.9 shows the graph of total pressure variation across the radial distance of the cyclone. The profile is generated at an axial position of y = 0.25 D with the incoming standard speed of U_o = 15 m/s. The Total pressure variation for all the tested geometries are shown in the graph.

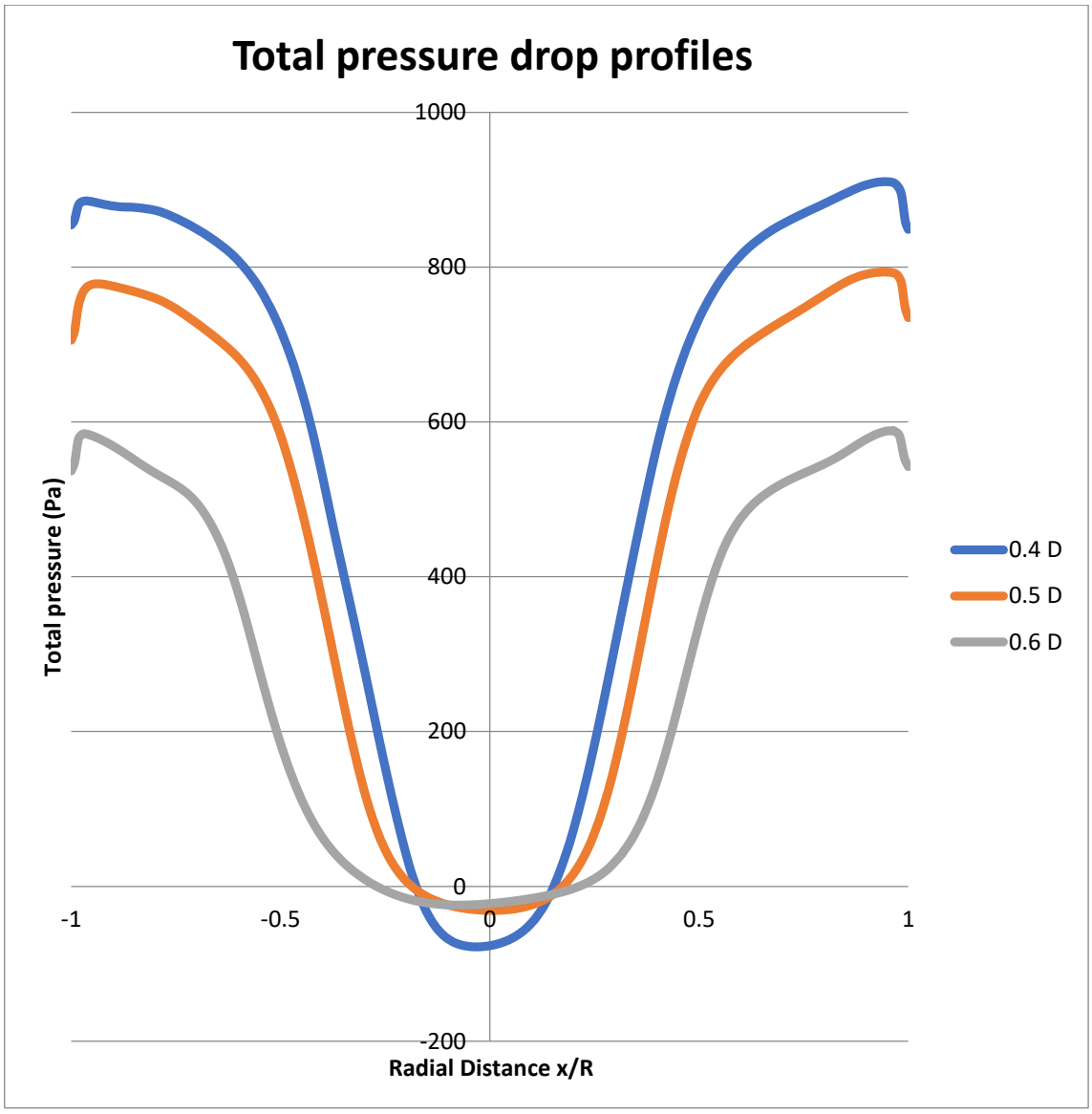

Figure 4.9: Graph showing Total pressure variation of the tested geometries at axial position of y= 0.25 D

It can be stated from the above graph that the total pressure drop trough the cyclone increases with decreasing the vortex finder diameter and vice versa. The profiles are in similar trend with the static pressure. The peak value of total pressure is the highest near the wall and lowest at the centre. Highest and lowest values of total pressure is attained for the 0.4 D vortex finder geometry i.e., 910.29 Pa and 77.865 Pa respectively. The reason of this is same as for static pressure profiles, the tangential velocity being the maximum for 0.4 D geometry and smallest for the 0.6 D geometry. The negative pressure in the middle of the geometry is highest for smaller diameter vortex finder because of high suction and swirl generation which revolves in the opposite direction. It is responsible for throwing out the clean air. Figure 4.10 shows contours of Total pressure drop through the cyclone geometries.

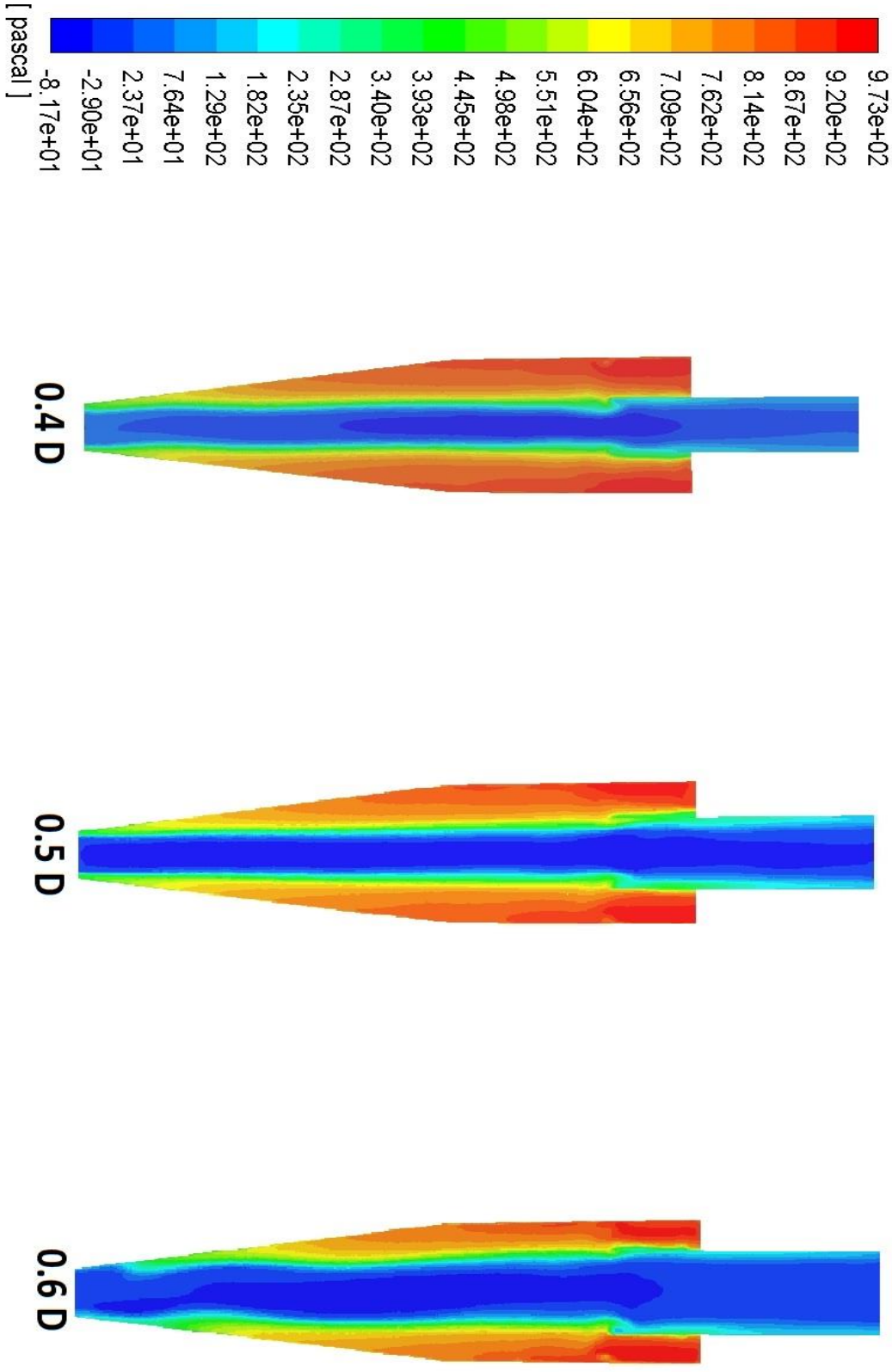

Figure 4.10: Contours of Total Pressure Drop through the cyclone geometries.

4.5 COLLECTION EFFICIENCY

The cyclone collection efficiency of the cyclone is the most vital parameter of its performance. It is considered as a function of vortex finder diameter. Collection efficiency is normally more difficult to predict because it depends largely on particle size distribution from the incoming parcel. **Grade efficiency curve** used to represent the Collection efficiency of cyclone separator. Collection efficiency is evaluated in this study by discharging a fixed number of single particles from the inlet of the cyclone and counting the number escaped and trapped particles from the outlet 1 and outlet 2 respectively. Collisions between particles and cyclone walls is presumed as perfectly elastic i.e., e=1. Also the collision between particles was not considered.

The main aim of this work is to examine the behaviour of cyclone separator on particulate matter separation from the incoming particle laden gas. Cyclone separator is basically used as a pre-cleaner and less efficient with small size of particles. To examine the collection efficiency of cyclone separator towards particulate matter is a complex procedure and many hit and trial methods were conducted to study the efficiency more precisely.

To simulate and track the particles through the cyclone, **discrete phase model (DPM)** is used along with RSM model. Coupling is the phenomenon of exchange of mass, momentum and energy between the phases. The particles have negligible effects on turbulence as the values of dispersed-phase volume fraction less than 10^{-6}. This is termed as one-way coupling. The volume fraction of particulate matter we are dealing with in the present work is much less than 10^{-6} and hence one-way coupling is assumed. The collection efficiency mainly depends on 2 factors:

- Pressure drop
- Tangential velocity

More the pressure drop and tangential velocity across the cyclone, more is the collection efficiency. Strong centrifugal and pressure profiles are generated where these two factors dominates. The formula for calculating the collection efficiency in this study is taken as follows:

$$\eta = \frac{\text{Particles trapped} - \text{incomplete particles}}{\text{Total tracked particles}}$$

With the help of the above formula, collection efficiency of different particles is calculated. The grade efficiency curves are given in figure 4.11 and 4.12.

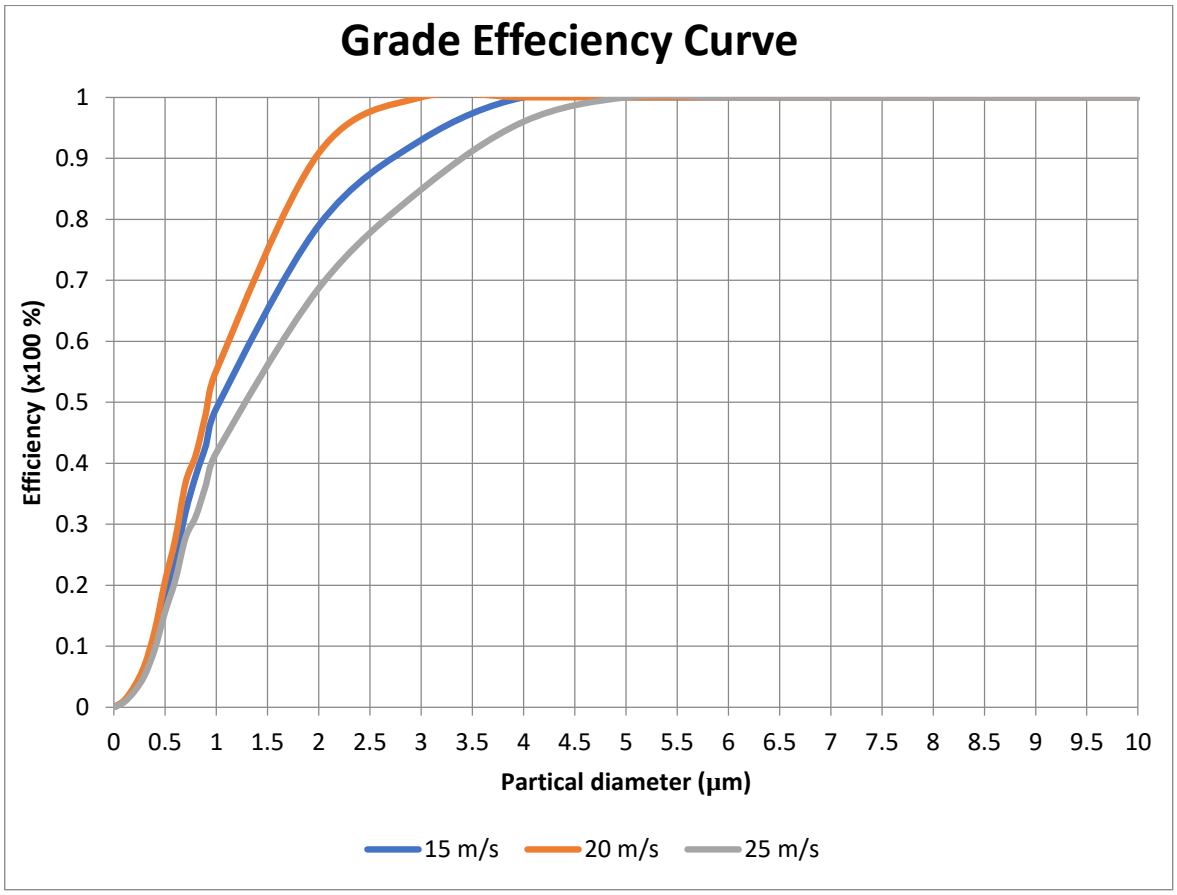

Figure 4.11: Graph of grade efficiency curve for standard Stairmand design (D_x= 0.5 D) at variable inlet velocities of 15, 20, 25 m/s

The mass flow rate is kept as $2x10^{-10}$ kg/m^3 from all the tested models. The particles are dispersed uniformly at inlet and inserted with velocity equals to the inlet flow. Figure 4.11 shows the numerical results of grade efficiency curve for standard Stairmand design at inlet velocities of 15, 20 and 25 m/s and particle density is taken as 2750 kg/m^3. The graph shows that with increasing inlet velocity, an increase in the collection percentage occurs. It is caused by the increase in the centrifugal force acting on the particles due to high tangential velocity.

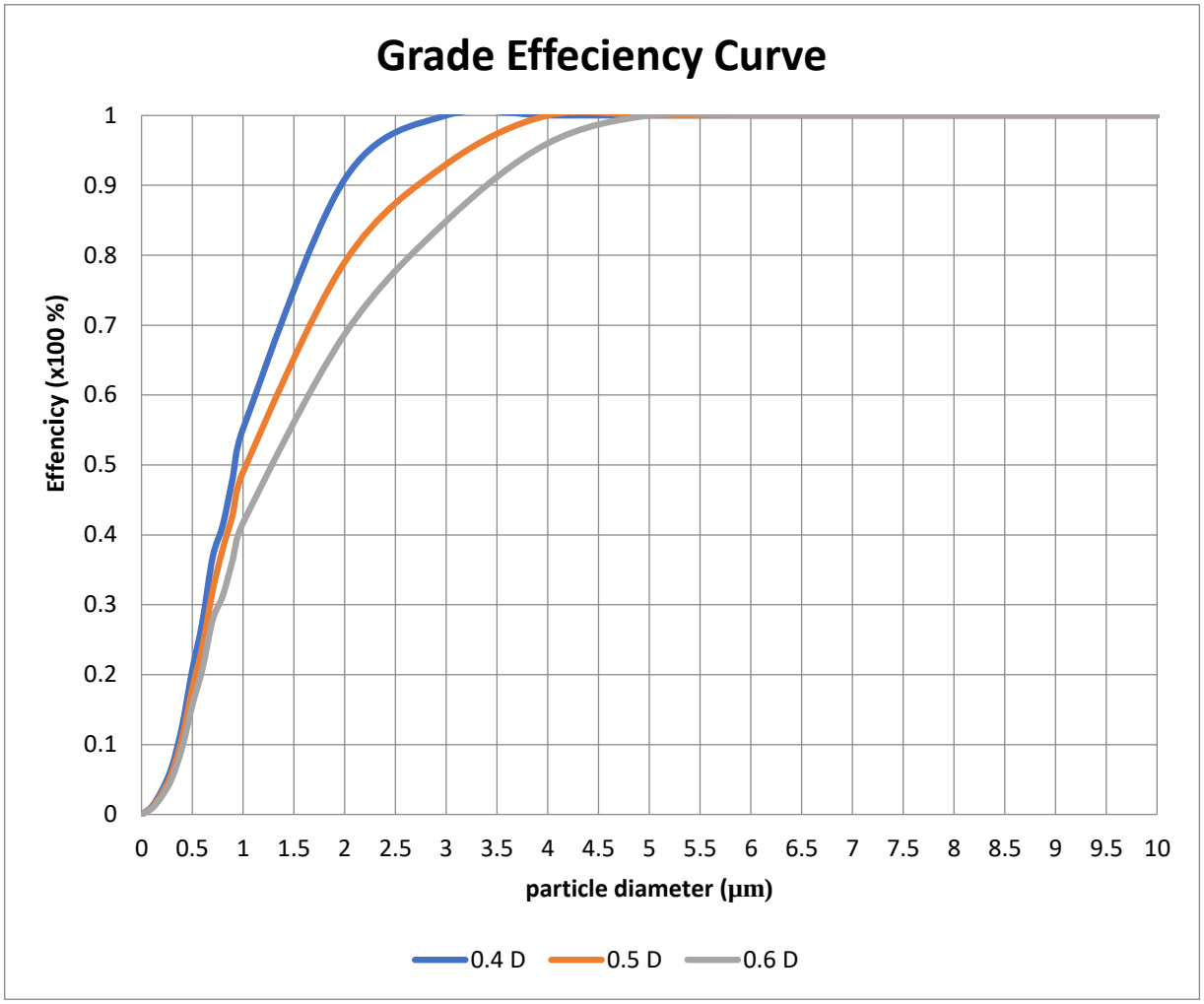

Figure 4.12: Graph of grade efficiency curve for all the three models (Dx =0.4 D,0.5 D,0.6 D)

Figure 4.12 shows the effect of vortex finder diameter on the collection efficiency when the inlet velocity is kept constant at 15 m/s. The curve shows that for a specific particle size, decreasing the vortex finder diameter increases the cyclone collection efficiency. It is due to the fact that the increase in tangential velocity and centrifugal force with decreasing the vortex finder diameter.

CHAPTER 5

CONCLUSION AND FUTURE SCOPE

5.1 Conclusion

A numerical technique based on CFD approach is used in this work to study the flow of air and particles through cyclone. Reynolds Stress Model (RSM) methodology is used to predict the turbulence behaviour of the flow and Discrete Phase Model (DPM) is used to predict the particle trajectories through cyclone separator. All the dimensional parameters of cyclone is kept constant except the diameter of vortex finder. Three cyclone models with different vortex finder diameters have been simulated using RSM methodology to study the effect of vortex finder diameter on the performance and flow pattern of the cyclone separator. The most significant conclusion of this study is the numerical techniques of CFD approach can be used to predict the flow parameters through the cyclone. This fact is clarified by the similarity obtained between the results of present study and published literature. Following conclusions can be drawn from the investigation:

- The maximum tangential velocity in the cyclone increases with decreasing the vortex finder diameter and vice versa.

- Decreasing the vortex finder diameter gradually increases the axial velocity through the cyclone and vice versa. Also, the axial velocity profile changes from the inverted W to the inverted V profile.

- Increasing vortex finder diameter reduces the pressure drop through the cyclone and vice versa.

- Increasing the vortex finder diameter reduces the collection efficiency for particulate matter and vice versa.

- Increasing the inlet velocity increases the collection efficiency of cyclone separator for particulate matter.

- Optimization of cyclone separator model is possible using numerical techniques of CFD approach.

5.2 Future Scope

As a recommendation of future work, the same study can be performed with different approaches and models. Many optimization techniques can also be used to increase the cyclone separator performance and efficiency. Some of the possible scope is given as points which are as follows:

- Use of Large Eddy Simulation methodology (LES) instead of Reynolds Stress Model (RSM) to predict the turbulent behaviour of cyclone.
- Altering the length along with diameter of the vortex finder.
- Altering various other dimensional parameters of cyclone separator like barrel diameter, cone tip diameter and inlet width.
- Effect of dustbin shape on overall performance
- Designing a new optimized geometry by considering all the significant parameters which will be more suitable for particulate matter separation
- Using different densities of particles and mass flow rates.

REFERENCES

[1]. C. B. Shepherd and C. E. Lapple. Flow pattern and pressure drop in cyclone dust collectors cyclone without intel vane. Industrial & Engineering Chemistry, 32(9):1246–1248, September 1940.

[2]. R. M. Alexander. Fundamentals of cyclone design and operation. In Proceedings of the Australian Institute of Mineral and Metallurgy, number 152, pages 203–228, 1949.

[3]. M. W. First. Cyclone dust collector design. ASME Annual General Meeting, Paper No. 49A127 (1949).

[4]. C. J. Stairmand. The design and performance of cyclone separators. Industrial and Engineering Chemistry, 29:356–383, 1951.

[5]. W. Barth. Design and layout of the cyclone separator on the basis of new investigations. Brennstow-W¨aerme-Kraft (BWK), 8(4):1–9, 1956.

[6]. A. Avci and I. Karagoz. Theoretical investigation of pressure losses in cyclone separators. International Communications in Heat and Mass Transfer, 28(1):107–117, 1 2001.

[7]. B. Zhao. A theoretical approach to pressure drop across cyclone separators. Chemical Engineering Technology, 27:1105–1108, 2004.

[8]. B. Zhao and Y. Su. Particle collection theory for cyclone separators: summary and comparison. Particle & Particle Systems Characterization, 23:484–488, 2006.

[9]. Karagoz and A. Avci. Modelling of the pressure drop in tangential inlet cyclone separators. Aerosol Science and Technology, 39(9):857–865, 2005.

[10]. J. Chen and M. Shi. A universal model to calculate cyclone pressure drop. Powder Technology, 171(3):184 – 191, 2007.

[11]. P. K. Swamee, N. Aggarwal, and K. Bhobhiya. Optimum design of cyclone separator. American Institute of Chemical Engineers (AIChE), 55(9):2279–2283, 2009.

[12]. D. C. Wilcox. Turbulence Modeling for CFD. DCW Industries, Inc, 2nd ed. edition, 1994.

[13]. J. Casal and J. M. Martinez-Benet. A better way to calculate cyclone pressure drop. Chemical Engineering, 90(2):99–100, 1983.

[14]. G. Ramachandran, D. Leith, J. Dirgo, and H. Feldman. Cyclone optimization based on a new empirical model for pressure drop. Aerosol Science and Technology, 15:135–148, 1991

[15]. D. L. Iozia and D. Leith. Effect of cyclone dimensions on gas flow pattern and collection efficiency. Aerosol Science and Technology, 10(3):491–500, 1989.

[16]. K. Rietema. Het mechanisme van de afscheiding van fijnverdeelde stoffen in cyclonen (in dutch). De Ingenieur, 71(39):ch59–ch65, 1959.

[17]. J. Dirgo and D. Leith. Cyclone collection efficiency: Comparison of experimental results with theoretical predictions. Aerosol Science and Technology, 4:401–415, 1985.

[18]. A. J. Hoekstra. Gas flow field and collection efficiency of cyclone separators. PhD thesis, Technical University Delft, 2000.

[19]. A.J. Hoekstra, J. J. Derksen, and H. E. A. Van Den Akker. An experimental and numerical study of turbulent swirling flow in gas cyclones. Chemical Engineering Science, 54:2055–2065, 1999.

[20]. C. Hoffmann, M. de Groot, W. Peng, H. W. A. Dries, and J. Kater. Advantages and risks in increasing cyclone separator length. AIChE Journal, 47(11):2452–2460, 2001

[21]. F. Boysan, W.H. Ayer, and J. A. Swithenbank. Fundamental mathematical-modelling approach to cyclone design. Transaction of Institute Chemical Engineers, 60:222–230, 1982.

[22]. W. D. Griffiths and F. Boysan. Computational fluid dynamics (CFD) and empirical modelling of the performance of a number of cyclone samplers. Journal of Aerosol Science, 27(2):281–304, 1996.

[23]. J. Gimbun, T.G. Chuah, A. Fakhru'l-Razi, and T. S. Y. Choong. The influence of temperature and inlet velocity on cyclone pressure drop: a CFD study. Chemical Engineering & Processing, 44(1):7–12, 2005

[24]. B.E. Saltzman and J.M. Hochstrasser. Design and performance of miniature cyclone for respirable aerosol sampling. Environmental Science & Technology, 17(7):418–424, July 1983.

[25]. J. C. Kim and K. W. Lee. Experimental study of particle collection by small cyclones. Aerosol Science and Technology, 12:1003–1015, 1990.

[26]. M. E. Moore and A. R. McFarland. Performance modeling of singleinlet aerosol sampling cyclones. Environmental Science and Technology, 27(9):1842–1848, September 1993.

[27]. K. S. Lim, H. S. Kim, and K. W. Lee. Characteristics of the collection efficiency for a cyclone with different vortex finder shapes. Journal of Aerosol Science, 35(6):743–754, 2004.

[28]. Raoufi, M. Shams, M. Farzaneh, and R. Ebrahimi. Numerical simulation and optimization of fluid flow in cyclone vortex finder. Chemical Engineering and Processing, 47:128–137, 2008.

[29]. G. Ravi, Santosh K. Gupta, and M. B. Ray. Multiobjective optimization of cyclone separators using genetic algorithm. Ind. Eng. Chem. Res., 39:4272–4286, 2000.

[30]. H. Safikhani, A. Hajiloo, M.A. Ranjbar, and N. Nariman-Zadeh. Modeling and multi-objective optimization of cyclone separators using CFD and genetic algorithms. Computers & Chemical Engineering, 35(6):1064–1071, 2011.

[31]. S. I. Pishbin and M. Moghiman. Optimization of cyclone separators using genetic algorithm. International Review of Chemical Engineering (I.RE.CH.E.), 2(6):683–690, 2010.

[32]. A. C. Coello, G. B. Lamont, and D. A. Van Veldhuizen. Evolutionary Algorithms for Solving Multi-Objective Problems. Springer, 2nd edition, 2007.

[33]. K. Elsayed and C. Lacor. Modeling, analysis and optimization of aircyclones using artificial neural network, response surface methodology and CFD simulation approaches. Powder Technology, 212(1):115–133, 2011.

[34]. K. Elsayed and C. Lacor. Multi-objective optimization of gas cyclone based on CFD simulation. In ECCOMAS thematic conference, CFD & Optimization, Antalya, Turkey, 23-25 May 2011.

[35]. B. Singer, Modeling the transition region, NASA report, NASA CR-4492, 1993

[36]. [36]. B.E. Launder, D.B. Spalding.The numerical computation of turbulent flows Comput. Methods Appl. Mech. Eng., 3 (1974), pp. 269-289